CHALMERS
UNIVERSITY OF TECHNOLOGY

Semi-Physical Modelling Approach for Exhaust Aftertreatment System of Heavy Duty Diesel Engines

Master's Thesis Report
Master's Thesis in Innovative and Sustainable Chemical Engineering

Author
Badhri Narayanan

Examiner
Jonas Sjöblom
Supervisors
Ali Ghanaati
Ethan Faghani
Jonas Sjöblom

Department of Chemistry and Chemical Engineering
Chalmers University of Technology
Gothenburg, Sweden 2018

Master's thesis 2018:62

Semi-Physical Modelling Approach for Exhaust Aftertreatment System of Heavy Duty Diesel Engines

Badhri Narayanan Ankam Sekhar

CHALMERS
UNIVERSITY OF TECHNOLOGY

Department of Mechanics and Maritime Sciences
Chalmers University of Technology
Gothenburg, Sweden 2018

Semi-Physical Modelling Approach for
Exhaust Aftertreatment System of
Heavy Duty Diesel Engines Badhri Narayanan Ankam Sekhar

Supervisor: Dr. Ali Ghanaati, Department of Mechanics and Maritime Sciences
Supervisor: Dr. Ethan Faghani, Project Manager, Volvo Penta
Supervisor: Professor Jonas Sjöblom, Department of Mechanics and Maritime Sciences

Examiner: Prof. Jonas Sjöblom, Department of Mechanics and Maritime Sciences

Master's Thesis 2018:62
Department of Mechanics and Maritime Sciences
Chalmers University of Technology
SE-412 96 Gothenburg
Telephone +46 31 772 1000

Cover: Muffler of a D13 Heavy Duty Diesel Engine

Typeset in LaTeX
Gothenburg, Sweden 2018

Semi-Physical Modelling Approach for an Exhaust Aftertreatment System of Heavy Duty Diesel Engines

Badhri Narayanan Ankam Sekhar
Department of Mechanics and Maritime Sciences
Chalmers University of Technology

Abstract

The aim of this thesis work was to establish a kinetic and heat transfer model for the Diesel Oxidation Catalyst (DOC) using GT-Suite. The kinetic model was calibrated using a transient Part Load Map (PLM) driving cycle. The inhibition functions of the reactions were tuned to obtain a good curve fitting of reaction species. When a different drive cycle was applied, the model predictability was poor. The result demands a requirement for better heat transfer modelling. A detailed external Heat transfer model was set up for this purpose. The results were better and the model was found to account for thermal mass variations in the system. The flow along the DOC was non-uniform, a 2 DOC model was established to account for the unequal inlet flow split and improved thermal mass understanding of the model. The results of the 2 DOC model however were inferred to be the same as 1 DOC. A discussion of results and a future outlook are presented.

Keywords: Catalyst Brick, Thermal Mass, DOC, EATS, Kinetic Modelling, Thermal Modelling, Heat Transfer, Inhibition Function

Acknowledgements

I would like to express my gratitude to Prof. Jonas Sjöblom for helping me throughout the course of this thesis. It was a fruitful experience to interact concepts and to learn the best practices followed in modeling and simulation.

I would like to thank Mr. Ethan Faghani, Chief Engineer at Volvo Penta for providing me with this opportunity. His insights and pragmatic approach towards problem solving helped me structure this project to provide meaningful results.

Thanks,
To all the countries I travelled by stories, ideas, laughs, misinterpretations, love.
To India, Germany, Austria, Hungary, Slovakia, Switzerland, Belgium, Italy, Netherlands, Croatia, Sweden, Norway, Finland.

To Alessia, for being such a friendly colleague, I enjoyed all the abstract lunch conversations we´ve had. It was fun to discuss ideas and solutions with her.

To all the people I had the chance to meet, either for a few words or for a few months.

To my parents,
To my love, Nami

Contents

1 Introduction **1**

1.1 Background 2
1.2 Literature 3
1.3 Objectives 4

2 Theory **5**

2.1 Mass and Heat Transport 5
2.2 Reaction Kinetics 7
2.3 Drive Cycles 8
2.4 Assumptions 9
2.5 Solver Theory 10

3 Methodology **11**

3.1 Modelling Approach 11
3.2 Model Setup 11
3.2.1 Physical Specifications 12
3.2.2 1 DOC Heat Transfer Model 14
3.2.3 2 DOC Heat Transfer Model 15
3.2.4 Activation Energy and Pre-exponential Factors 17
3.2.5 Integrated Design Optimizer 18

4 Results and Discussion **19**

4.1 Low Torque Region 19
4.2 Inhibition Functions 20
4.3 Steady State Points 22
4.4 Heat Transfer Model 23
4.5 2 DOC Model 29
4.6 Model Validation 33

5 Conclusion **37**

Bibliography **38**

A Appendix **II**

A.0.1 Results from Almqvist [1] II

A.0.2 Results from Cen [2] III

A.0.3 Matlab Program V

Introduction

Diesel Engines are predominantly used in heavy duty vehicles due to their reliability and efficiency. NO, CO and Hydrocarbons (HC) produced during combustion are harmful for the health [3]. The advent of catalytic exhaust aftertreatment systems have significantly reduced emissions. However, emission regulations for non-road vehicles are becoming more stringent every year, according to the Euro V regulation standards, the permissible limits for HC+NOx is 7.5 g/kWh and CO is 8 g/kWh [4]. Continuous improvements have been made by the automotive industry to develop testing and measurement rigs to understand the behaviour of systems but the resources and efforts that go into real-time physical testing are tremendous.

Model based prediction systems have proven to be a useful tool in EATS calibration and optimization. EATS models help study the effects of various system parameters with less effort and shorter time than an engine test cell [5].

Various EATS models have been established before but the accuracy of the models is questionable either due to the lack of predictability or the reproducibility of the model. Ideally, a model could have different set of kinetic parameters that would give equivalent results. However, it becomes hard to build a consistent model that would perform well in different drive cycles. Therefore, this thesis work concentrates on modifying an existing model to obtain an improved model with better accuracy and applicability across various engine drive cycles.

The EATS system transmits the exhaust gas into the environment. The system is concealed in a closed cabinet called the muffler to provide noise attenuation. The muffler is made of various materials such that they exhibit high mechanical strength and withstand high temperatures. Mild carbon steel with aluminum coating is typically used in the EATS systems to be protected from corrosion [6]. There are various design parameters considered while designing a muffler. One of the main functionality is to muffle down the noise, it is typically done by having a resonating chamber that reduced the sound pressure [7]. Generally, the muffler design is such that the exhaust gases are forced to pass through a series of geometric changes which causes a significant amount of backpressure. Backpressure has to be reduced to avoid power losses [7]. It is also equally challenging to have

the smallest muffler size and the lowest cost without sacrificing functionality.

1.1 Background

One of the primary parts of a vehicle's EATS system is the Diesel Oxidation Catalyst (DOC). CO and HC are oxidized into harmless gases (CO_2, H_2O). NOx compounds are reduced to N_2 in the Selective Catalytic Reduction (SCR) catalyst which is located later in the EATS system. A good NO_2:NO ratio is proven to improve the conversion efficiency of the SCR and a modern DOC setup supports it by converting NO into NO_2 [6].

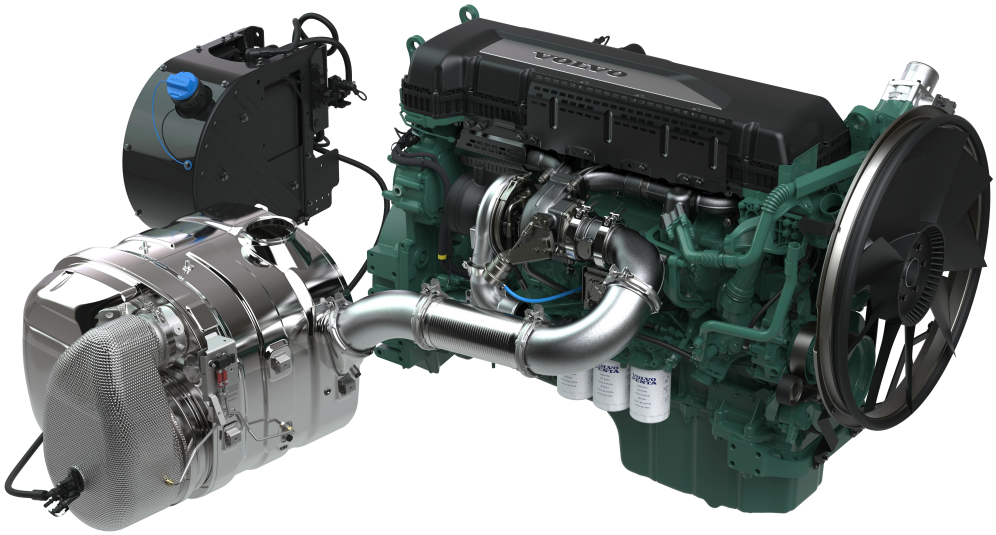

Figure 1.1: A Volvo Penta stage V D13 Engine connected to an Exhaust After Treatment System (EATS) with a Urea tank

The Euro VI emission standards noted that reduction in NOx from diesel engines were necessary for maintaining the air quality [8]. Portable Emission Measurement System (PEMS) were mounted onboard to quantify the unexpected rise in NOx levels and it was found that the NOx reductions were insufficient. It was further concluded that this was because the NEDC drive cycle used to gaugue the emissions did not capture the full range of the load map [8]. Hence, In this study a Part Load Map (PLM) driving cycle is used due to is highly transient nature.

VIRTEC (VIrtual TEst Cell) is a test rig which is a computer based engine testing cell designed by Volvo Penta, where a virtual engine is setup and its behaviour is simulated using computer aided tools. The objective of this thesis work is to establish a model to predict the Exhaust After-Treatment System (EATS) species of a heavy duty D13 diesel engine based on material specifications and inlet data only. This would drastically minimize the cost and effort put into physical measurements and testing. In this project, a 1D reactor model is designed and the heat, mass and reaction kinetics parameters are calibrated to provide good data predictability for various commonly prevalent engine drive cycles. The model has to be integrated with other virtual engine components and hence has to be robust in terms of accuracy, stability and speed.

The reactions in the DOC system are highly temperature sensitive. The flow through this particular system of study is not uniform, thus making the modelling process more complex and challenging. The scope of this thesis work is hence to develop a GT-Suite model that would be capable of accurately predicting exhaust aftertreatment performance for various engine driving cycles. A detailed thermalmass model will be established, the obtained results will then be calibrated against measured dataset to obtain a better fit. Later, a validation of the model will be performed over a different engine driving cycle and further improvements will be done. Further, an approach for modelling the non-uniform flow behaviour will also be presented.

1.2 Literature

This similar problem has been tackled by multiple researchers before. A genetic algorithm was developed by Hansen et al. in Matlab [9]. The pre-exponential factor and activation energies for 10 reactions were simultaneously optimized. There was a difference of at most 10% in the conversion prediction. Forsthuber et al. established a 1D combustion model to evaluate tail pipe emissions, the prediction was still worse by a 100 ppm of species concentration [4]. Katare et al. established a hybrid DOC model with kinetic and statistical tools [10]. A good data fit was observed however the model accuracy fell by +-5 % when it was validated against data of different fuel injection rates. A QS modelling approach was taken by Tang et al. where a solver was setup for heat and mass transport calculations along different regions of the system [11]. This model was observed to have a good predictability.

Tremendous amount of research has been conducted in EATS modelling before, but they seem to be either empirical and system specific or lack physical insight. In general, most of these models even if they have good predictability, seem to fail when a varied set of driving cycles are applied. This is due to the fact that the model is built and tuned only to handle dataset within a particular range of operating conditions. This thesis work hence concentrates on producing a good and an efficient model that would perform well in most practical engine operating scenarios.

1.3 Objectives

The key objectives of this thesis work are:

- Establish a 1D GT-Suite model to predict the behaviour of temperature and reaction species concentration in a DOC
- Establish a detailed Heat Transfer model to capture the thermal mass variations of the system
- Improve the model interms of model predictability and applicability across various drive cycles
- Validate the feasibility of the model against a Non-Road Transient Cycle (NRTC) drive cycle
- Develop a model to account for the flow maldistribution in a DOC

Theory

The Diesel Oxidation Catalyst (DOC) is the first component of a typically used automotive Exhaust Aftertreatment System (EATS). The primary goal of the DOC is to reduce the amount of CO by oxidation using catalysts such as PGM.

2.1 Mass and Heat Transport

The exhaust gas flows axially through the monolith while the mass and heat transport occurs both in the axial and radial direction.

According to the Two film theory [12], the catalytic process in heterogeneous catalysts happen through the following steps:

1. There exists a boundary layer between the catalyst surface and the bulk gas as the gas starts flowing through the reactor.
2. Transport in axial direction occurs through convection
3. The reaction species in the bulk of the gas diffuses radially to the boundary layer. This is called external diffusion
4. When the species are on the surface of the catalyst, surface reactions take place.
5. The reaction species on reaching the surface of the catalyst site, further diffuse through the pores structure in the catalyst. This is called internal diffusion
6. The formed product diffuses out to the bulk gas along the same path.

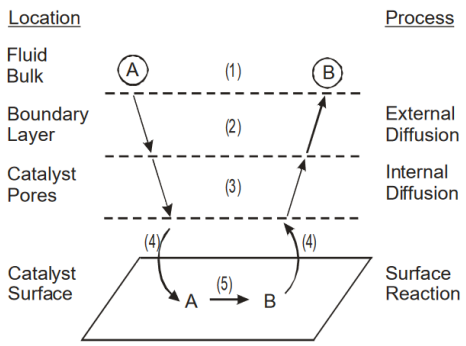

Figure 2.1: The 2 Film theory explaining the flow of reaction species to and from the catalyst site [12]

The other governing equations as followed by Gamma Technologies [13] are:

Solid Phase Energy:

$$\psi_s \frac{\partial T_s}{\partial t} = \frac{\partial}{\partial z}(f_{sb}\lambda_{sb}\frac{\partial T_s}{\partial z} + hS(T_g - T_s) - \sum_{j=1}^{nrct} \Delta H_j r_j + \frac{P}{V} + h_x S_x(T_x - T_s)) \quad (2.1)$$

Gas Phase Energy:

$$\epsilon \rho_g u C_{pg} \frac{\partial T_g}{\partial z} = hS(T_s - T_g) \quad (2.2)$$

Continuity:

$$\frac{\partial}{\partial z}(\rho_g \nu) = 0 \quad (2.3)$$

Momentum:

$$\epsilon \frac{\partial p}{\partial z} + \epsilon \rho_g \nu \frac{\partial \nu}{\partial z} = -Sf\frac{1}{2}\rho_g \nu^2 \quad (2.4)$$

The boundary condition at the surface connects the washcoat solution to the channel gas problem, at x=0:

$$\rho_s D_{e,i} \frac{\partial \omega_i}{\partial x} = k_{m,i}(\omega_i - \omega_{g,i}) \quad (2.5)$$

The heat and mass transfer coefficients are related to a single Nusselts number. The Nusselt Number is a constant and it is based on the assumption that the channel flow rate is laminar and well-understood. It is calculated using the equation

$$h = Nu\frac{\lambda_g}{D_h} \quad (2.6)$$

$$k_{m,i} = Sh\frac{\rho_g D_{i,m}}{D_h} \quad (2.7)$$

The dependant variables mentioned above are determined by

$$\sum_k \theta_k = 1(foreachsite) \quad (2.8)$$

$$A_k \frac{\partial k}{\partial t} = \sum_j \sigma_{kj} a_j r_j \quad (2.9)$$

$$\epsilon \rho_g \nu \frac{\delta \omega_i}{\delta z} = k_{m,i} S(\omega_{s,i} - \omega g, i) \quad (2.10)$$

2.2 Reaction Kinetics

The basic reactions that occur in a DOC are Eqn (2.13-2.17). The global kinetics mechanism was followed as suggested by Voltz [14] with improvements suggested by Khosravi et.al [15]. At low temperatures the chemisorption of HC and CO species are more favoured while the surface coverage pattern shifts as the temperature increases. This phenomenon is vice versa for NOx adsorption and desorption [16]. This emphasizes on the need for a temperature specific model that would capture variations in different temperature domains. As Almqvist [1] and Cen [2] discussed in their thesis works, the activation energy and pre-exponential factors for reactions involved were observed to be different in different research papers. Hence, a system specific reaction kinetics model for different temperature domains was developed.
The rate of reactions are typically modelled using Langmuir Hinshelwood reaction mechanisms Eqn 2.11 shows the basic reactions involved in the DOC
The rate constant k take the Arrhenius form:

$$k = Aexp^{\frac{-E_a}{RT}} \tag{2.11}$$

Reaction rates are solved using local gas concentrations in the washcoat surface. The overall rate of the reaction is calculated using:

$$r = \frac{k[concentration]^{order}}{G(i)} \tag{2.12}$$

$$CO + 0.5O_2 \longrightarrow CO_2 \tag{2.13}$$

$$C_3H_6 + 4.5O_2 \longrightarrow 3CO_2 + 3H_2O \tag{2.14}$$

$$NO + 0.5O_2 \longrightarrow NO_2 \tag{2.15}$$

$$DF + 19.4O_2 \longrightarrow 13.5CO_2 + 11.8H_2O \tag{2.16}$$

$$H_2 + 0.5O_2 \longrightarrow H_2O \tag{2.17}$$

Due to the complex nature of diesel fuel, the composition of diesel fuel was approximated to 40% propylene, 30% hydrocarbons adsorbed onto the catalyst surface and 30% hydrocarbons present in the gas phase. This proportion was obtained from observations and recommendations made by Sampara [16] and Almqvist

[1]. The mole fractions of H_2, H_2O, propylene and diesel fuel were calculated according to Eqn 2.18-2.19 based on recommendations made by Gamma Technologies

$$[Propylene] = \frac{[HC].0.4}{3} \qquad [DieselFuel] = \frac{[HC].0.3}{13.5} \tag{2.18}$$

$$[H_2] = \frac{[CO]}{3.5} \qquad [H_2O] = [CO_2] \tag{2.19}$$

Reactions in DOC are highly competitive. Voltz [14] introduced the concept of inhibition functions which are non linear terms that the rate expression is divided by. These functions pave way for accurately tuning the simulation curves to best match the measured data in model based prediction.

$$\begin{aligned} r_{CO} &= k_{CO}\frac{[CO].[O_2]^{0.5}}{G(1)G(2)} \\ r_{NO} &= k_{NO}\frac{([NO].[O_2]^{0.5} - [NO_2])G(4)}{G(2)G(3)G(5)} \\ r_{prop} &= k_{prop}\frac{[Propylene].[O_2]}{G(1)G(2)} \\ r_{DF} &= k_{DF}\frac{[DF].[O_2]}{G(1)G(2)} \end{aligned} \tag{2.20}$$

$$\begin{aligned} COinhibition : G(1) &= (1 + [A_{COinh}].exp^{\frac{[Ea_{COinh}]}{T}}[CO])^2 \\ HCinhibition : G(2) &= (1 + [A_{HCinh}].exp^{\frac{[Ea_{HCinh}]}{T}})([DF_{ads}] + [DF_{vap}])^2 \\ NOinhibitionG(3) &= 1 + [A_{NOinh}.exp^{\frac{[Ea_{NOinh}]}{T}}[NO] \\ Conversionfactor fromK_{eq}toK_c &= \sqrt{\frac{101325}{R.T}} \\ NOOxidationequilibriumconstantK_{eq} &= 1.510^{-4}exp^{\frac{6864}{T}} \end{aligned} \tag{2.21}$$

2.3 Drive Cycles

Inorder to have a global model that would be capable of performing equally well at all exhaust flow conditions, the engine is exerted in almost all possible ways such as to replicate all possible practical vehicle operating scenarios. Engine drive cycles are widely used in assessing the performance of an engine in various categories such as fuel consumption and emissions.

In this thesis, the Part Load Map (PLM) drive cycle will be used to develop the kinetic model since the variations in operating conditions are highly transient. The heat transfer model will be developed using the C1 drive cycle. Model validation will later be performed in the Non-Road Transient Cycle (NRTC).
Fig. 2.2 shows the torque and speed map of various drive cycles

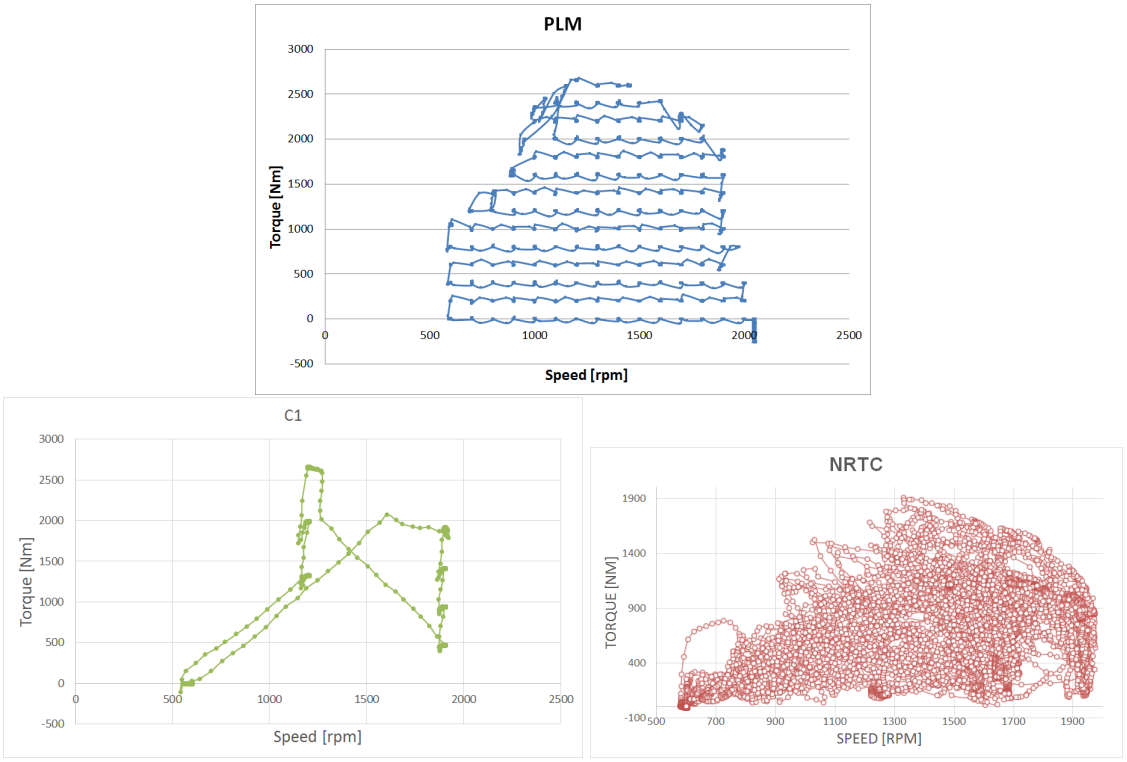

Figure 2.2: The Torque and Speed map for PLM, C1 and NRTC driving cycles

2.4 Assumptions

- Axial mass and heat transport in the gas phase occurs through convection only
- Axial heat conduction along the monolith happens through conduction
- Heat transfer through radiation is negligible inside and outside the monolith
- Diffusion mass transfer was assumed to be negligible
- The pressure drop across the reactor is negligible
- Ideal gas behaviour.

2.5 Solver Theory

GT-Suite considers quasi steady approximation when the QS flow solver is used. This is due to the short residence time of exhaust gas through the reactor. QS solver can resolve large time steps for faster computational time.

The 'Advanced Adaptive' chemistry solver was used to solve chemical equations. This solver is based on an adaptive mesh methodology and uses numerical methods specifically designed for catalytic reactors [13].

The catalyst wall temperature is automatically calculated by the QS solver. In-order to have a smooth wall temperature profile, the catalyst brick is internally discretized into small tanks. Based on practice, a smooth wall temperature profile was obtained for a discretization length of 5mm.

In the external heat transfer model, the solver is set to RADAU a 3 stage, 5th order DAE solver for numerical robustnuss and its improved ability to handle stiff kinetics and heat transport.

The frequency of measured data was 1s and hence a simulation time step of 1s was chosen to accurately model the transient flow behaviour.

The exhaust gas flow has reaction species concentration in the order of ppm. Hence, for better accuracy, the error tolerance was set to 1E-6.
The total error was calculated cumulatively, the difference between measured and predicted values were squared and added consecutively for each point as shown in the following equations

Total Absolute Error Function = $F_i \int_0^t (y_{measured} - y_{predicted})^2$

Total Relative Error Function = $F_i \int_0^t (\frac{y_{measured} - y_{predicted}}{max(abs(y_{measured}, 1E-17))})^2$ (2.22)
Where F_i is the weighting factor of species i.

Methodology

3.1 Modelling Approach

Typically the engine is tested under different drive cycles to exert the engine into a wide range of conditions inorder to determine its behaviour in a transient real life environment. A transient drive cycle called Part Load Map (PLM) was used to establish the kinetic model and the C1 cycle was used to establish the heat transport model. This model was later validated using NRTC drive cycle. Table 3.1 shows the test plan followed

Table 3.1: Test Plan for model building

Criteria	Calibration	Validation
Kinetic Parameters	PLM	NRTC
Heat Transfer Parameters	C1	PLM & NRTC

GT-Suite was used to model the 1D heat and mass behaviour. The reaction kinetic parameters from Almqvist´s model [1] were used as an initial guess. The thermal insulation layers in the catalyst brick was specified according to specifications obtained from Volvo Penta.

Reaction kinetics were tuned majorly using the Activation Energy and the Pre-exponential factors of important reactions in DOC. It could further be observed from Almqvist's model [1] that the predictability reduces at low temperatures. The reaction could be strongly inhibiting at these regions and hence the inhibition functions of all the major chemical reactions were tuned.

3.2 Model Setup

A GT-Suite 'Catalyst Brick' component was used to represent a DOC reactor. 'EndFlowInletSpecies' component was used to incorporate inlet flow conditions such as temperature, mass flow and concentration of the exhaust gas. The gas then passes through an inlet cone which expands the flow area to the DOC reactor. The gas then flows similarly out of the reactor to the outlet component as shown

in Fig 3.1. In-between components, the 'nocond' element is used to avoid heat dissipation along the pipes and connections. 'SurfaceReactions' component was used to implement reactions inside the DOC.

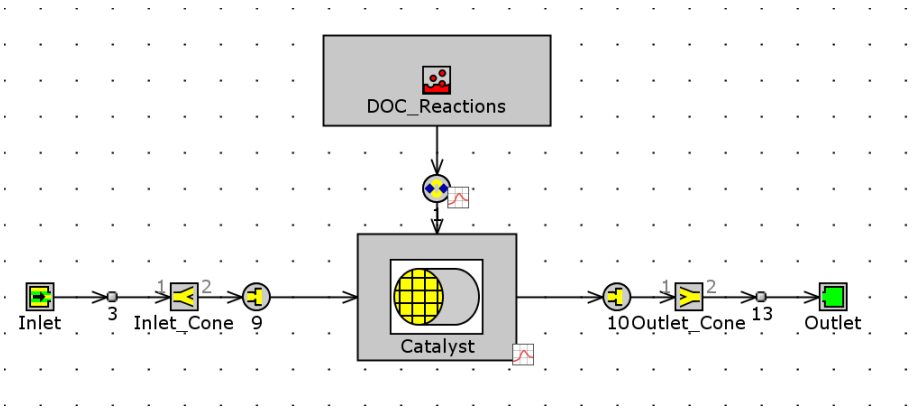

Figure 3.1: The GT-Suite DOC model with flow connections

3.2.1 Physical Specifications

The geometric specifications of the monolith was incorporated as provided by the supplier. The basic model has only 1 DOC catalyst brick with flow connections. The 'Calculated Wall Temperature' option was selected for GT-Suite to calculate a wall temperature in each tank. The DOC muffler contains several insulation layers consisting of different materials as shown in Fig 3.2, the thermal insulation layers were specified according to material property information given by supplier.

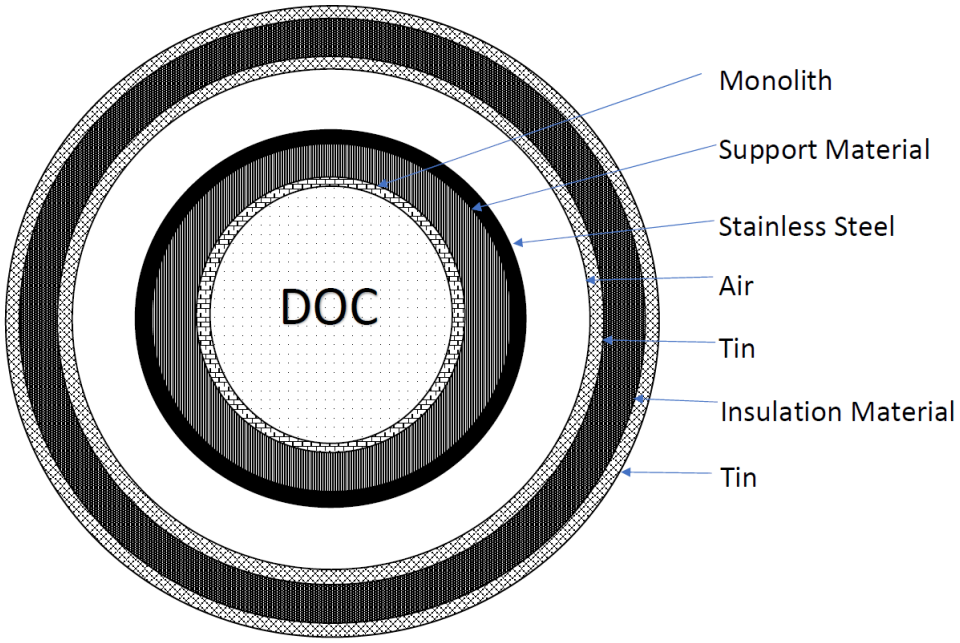

Figure 3.2: Thermal insulation layers surrounding the DOC to form the muffler

The active catalyst site specifications were obtained from the supplier and are not displayed here due to confidentiality reasons. The chemical reactions and the general inhibition terms were entered as discussed earlier. The geometric parameters of the catalyst brick and the muffler were entered as shown in Table 3.2.1

Table 3.2: Monolith and Insulation Layer specifications

Name	Value
Frontal Area	xx in^2
Reactor Length	xx in
Channel Shape	xx
Cell Density	xx cpsi
Washcoat Thickness	xx in
Support Material	xx mm
Stainless Steel	xx mm
Air gap	xx mm
Tin	xx mm
Insulation Material	xx mm

3.2.2 1 DOC Heat Transfer Model

The thermal mass variations along the reactor was modelled since the temperature predictions are poor interms of response and lag. An external heat transfer model was developed in GT-Suite to define the thermal interactions in the system.

Typically, 1D catalyst models are developed for fastness and simplicity. However, they only predict the fundamental axial behaviour of the catalyst channel and do not strictly account for the change in temperature, concentration and flow in the radial direction. It is thus not possible for 1D models to understand the thermal mass variations along the catalyst channels. To resolve the shortcomings of 1D catalyst models, an external heat transfer model (1D+1D) is hence developed to tune the thermal mass properties of insulation layers around the catalyst walls.

The system is highly temperature dependent and hence a detailed external heat transfer model was setup. GT-Suite has the flexibility to design each thermal insulation layer separately as 'Thermal primitives'. The mode of heat interaction between these layers has to be specified, as shown in the Fig 3.3. When external heat transfer model is setup, the solver calculates only 1 distinct wall temperature for a thermal connection. Based on practice and previous experience, a discretization length of 5mm produced a smooth wall temperature profile. Hence, the DOC reactor was split into 23 tanks (114.3/5=23) each of which is an axial-subvolume of 5mm long representing a reactor of total length 114.3mm as seen in Fig 3.4. The computational penalty in this model was high, but this method of modelling was observed to consider the thermal mass behaviour of the system and provided a better means to control it.

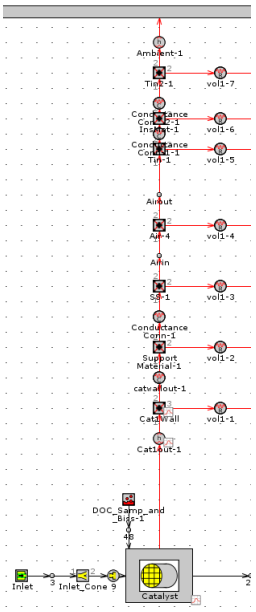

Figure 3.3: External Heat transfer model - GT-Suite representation with thermal connections

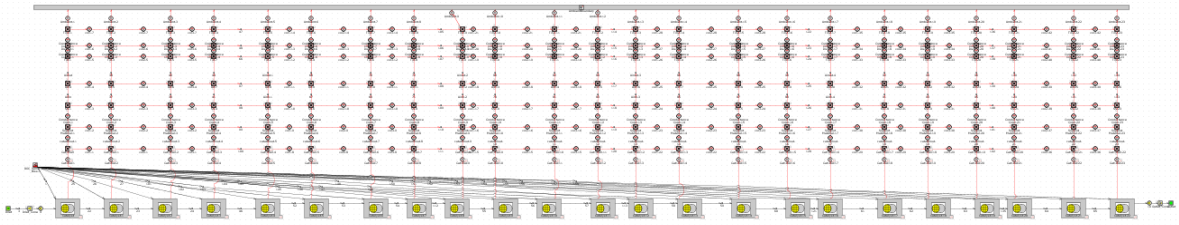

Figure 3.4: The 1 DOC model with 23 catalyst subvolumes and thermal connections

3.2.3 2 DOC Heat Transfer Model

According to Almqvist [1], there is flow maldistribution in the system under consideration. This phenomenon has to be accounted for since a real world system will almost always not have a uniform well-mixed flow. Fig 3.5 shows the distribution of flow in the DOC inlet. A 2 channel catalyst brick system is devised for this purpose to account for flow and heat distribution. In this fictitious model it is hypothesized that there is a large DOC and there exists a small DOC inside the large DOC which transfers heat between each other. This way, it is believed that the thermal mass heat up in the monolith could be more precisely modelled. Moreover, on looking at the flow maldistribution in Fig 3.5, it could be approximated that around 40% of the flow goes upward and the remaining goes downward. Hence, a distribution fudge factor α was devised to account for the discrepancy

in exhaust gas flow distribution. Fig 3.6 shows the GT-Suite model with 2 DOCs and heat exchange connections between them. According to this model, the flow is split into 0.4 (α) and 0.6 (1-α) times and sent into 2 different DOCs with similar geometric properties proportionally scaled by a ratio of α. This setup will by all means collectively represent the specifications of a single DOC reactor. Fig 3.7 shows a schematic representation of the model. By way of modelling 2 DOCs there is more scope for the solver to individually solve the poor flow regime section to obtain a more accurate solution in the nearly stagnant region.

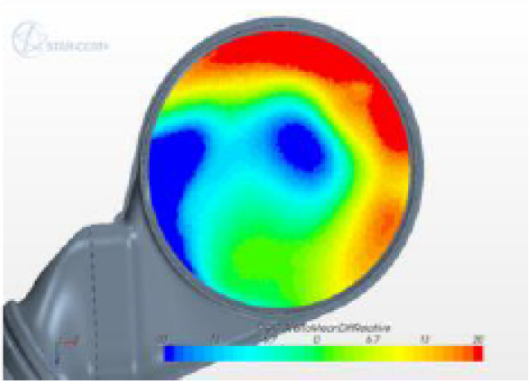

Figure 3.5: CFD simulation over inlet velocity to DOC. Blue indicates -20% of average velocity and red indicates +20% of average velocity.

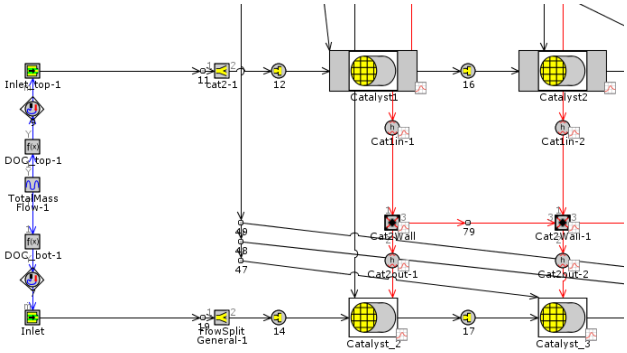

Figure 3.6: GT-Suite representation of the 2 DOC model

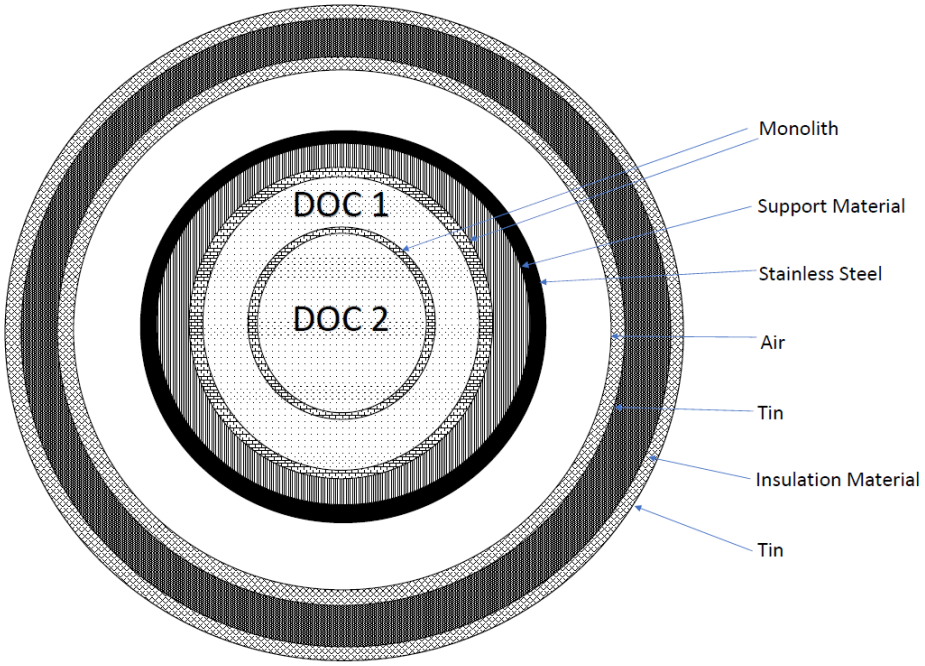

Figure 3.7: Front view schematic representation of the 2DOC model with insulation layers

3.2.4 Activation Energy and Pre-exponential Factors

There are 4 main reactions taking place in the DOC. The activation energy and the pre-exponential factors for each reaction were optimized.

The following working methodology was implemented. First, the pre-exponential factors alone were tuned. Then the pre-exponential and the activation energies while keeping the inhibition functions constant. Later all three terms were optimized together. This was performed inorder to get a good starting point for consequent optimization runs and also to account for interactions of these parameters one at a time.
After the heat transfer parameters were optimized, the kinetic parameters were re-optimized by following the same procedure as mentioned above.

3.2.5 Integrated Design Optimizer

The Integrated Design Optimizer (IDO) by GT-Suite is used to minimize the total error functions for temperature and species prediction.

Depending on the system, there could exist multiple local optima. It is often not possible to know the complexity of the system, since the point of convergence is dependent on the initial conditions given. GT-Suite however has sophisticated optimization search techniques to converge at a global minima. For optimization involving less than 3 independent parameters, the Simplex algorithm was used and for complex scenarios with more parameters, the Genetic Algorithm was used.

The genetic algorithm is particularly robust in searching the grid space for the point of global minimum. However, in a scenario where a good initial condition is not known or when multi-objective optimization runs are performed, the optimizer had to be run for multiple evolution until a satisfactory minimum was obtained.

GT-Suite also provides the ability to run parallel iterations. Tasks are equally distributed among different cores of the processor to simultaneously perform multiple iterations at a time. This reasonably reduces computational time when running large simulations.

To resolve this issue, 2 methods were followed. In the first method, every optimization run was first simulated to minimize absolute error and the obtained optimum values were used as an initial starting point to perform a 2nd optimization to minimize the relative error. In the second method, each species term was treated as an individual error term and was minimized using multi-objective optimization.

It is important to not have very small data points for the concentration terms. This could cause problems when minimising the relative error since the error term could be extremely large due to a low concentration point and the optimizer will be rendered incapable of judging the difference in error which may make it to lose feasible optimal parameters. For this purpose, data was processed for all the measured concentration terms entered in the total error function by removing the very small near zero values.

Results and Discussion

4.1 Low Torque Region

Fig 4.1 shows the PLM drive cycle low torque region. As marked in the figure, It could be noticed that the torque goes to 0 for certain speed conditions and sometimes also becomes negative. Almqvist's and Cen's models consistently had low predictability in exactly these regions. When drive cycle experiments are conducted, the engine is exerted in every possible manner inorder to observe the exhaust flow behaviour is all practical conditions. However, a negative torque implies that engine traction occurs and the engine runs in idle speed. The gas flow at this time is influenced by the prevailing flow conditions. Since the species prediction is bad exactly in this location, it is possible that this engine condition influences the exhaust flow.

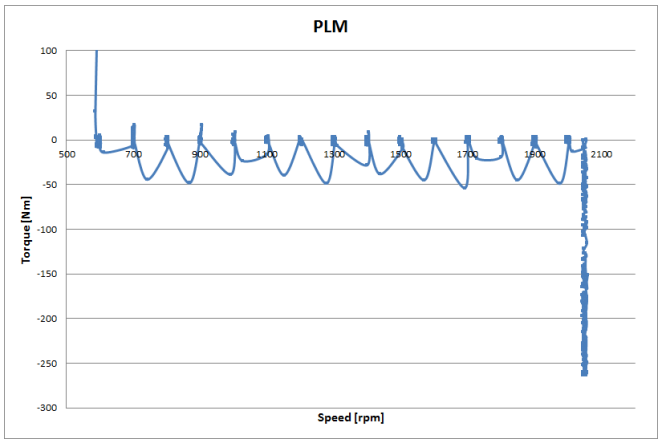

Figure 4.1: The PLM low Torque region showing the 0 and negative torque scenario

It it highly likely that the reaction species CO, NOx and HC go through the reactor untreated at these low temperature and low mass flow region above 24000s [17] Etheridge et. al noticed that kinetic parameters which predict the same behaviour when the temperature is increasing, give different predictions when the temperature is decreasing. Besides, if lower concentrations are encountered in the drive cycle than were used for kinetic development; kinetic parameters which give equivalent predictions at higher concentration may give different predictions at lower concentration [18].

4.2 Inhibition Functions

From Almqvist's results, Fig A.1, A.2, A.3 [1], it is clear that the species prediction becomes poor after 17000s. This was suspected to be due to the strong inhibiting nature of the chemical reaction. This was also noted to be the low temperature region and hence parametric optimization was performed only in the last 10000s. On tuning the inhibition functions, the species prediction has vastly improved as shown in Fig 4.2 , the NOx prediction above 17000s until 24000s has improved.

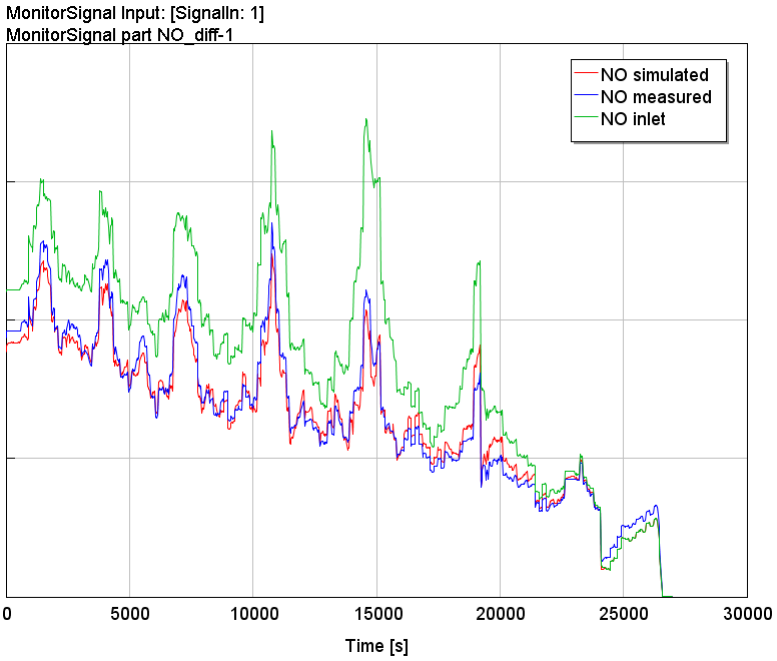

Figure 4.2: NOx flow along the reactor for a PLM dataset with improved inhibition functions

Although the predictability in the low temperature regions for CO and HC are maintained as shown in Fig 4.3, 4.4 it is still insufficient. Since the reactions in the DOC compete with one another, the rates of the reaction for HC and NO oxidation are highly interdependent. Hence, a detailed optimization has to be performed by defining the error terms individually for all the species and minimizing the error terms using multi-objective optimization.

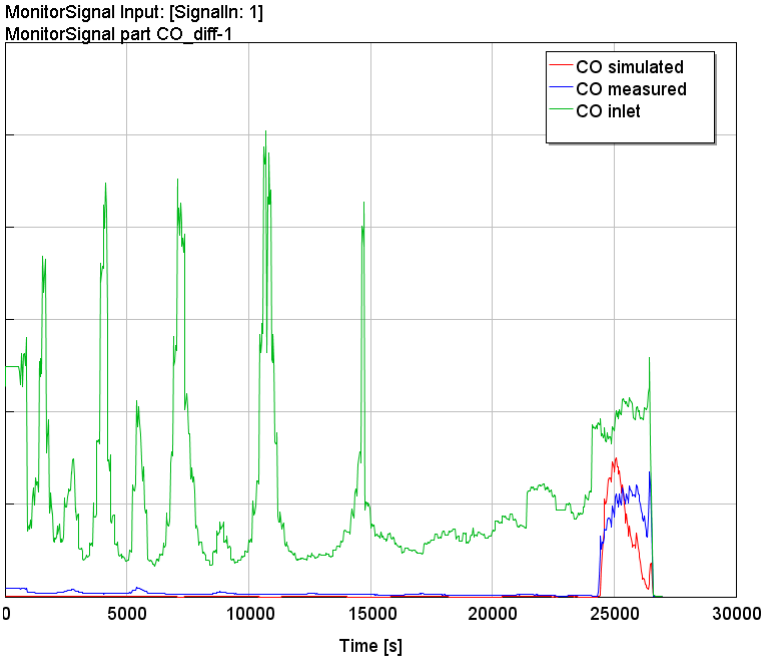

Figure 4.3: CO flow along the reactor for a PLM dataset with improved inhibition functions

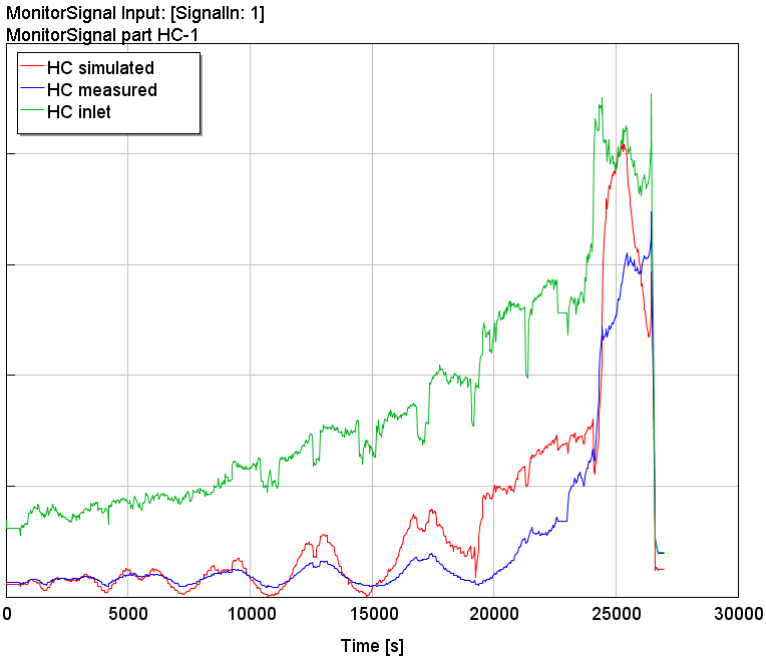

Figure 4.4: HC flow along the reactor for a PLM dataset with improved inhibition functions

Table 4.1: List of old and new parametric values of inhibition functions.

Parameter Name	Old Values	New Values
Ea HC inh	1.67 E4	1.7 E4
A HC inh	2.12 E-12	1.40 E-12
Ea CO inh	-1.49 E4	4.16 E4
A CO inh	248	24
Ea NO inh	5.7 E3	4.94 E3
A NO inh	0.25	0.94

4.3 Steady State Points

Inorder for the model to better understand the curve patterns, it was decided to calibrate the model for steady state (SS) data points of the PLM drive cycle and later use these parameters on the large PLM dataset. Hence, 90 steady state data points were obtained by averaging values every 300s and the kinetic parameters were tuned. The results improved, but the species predictions were still not satisfactory. As shown in Fig 4.5, the NOx prediction is better than Almqvist's model but isn't any better in comparison with the low temperature model as shown earlier. In general, from Fig 4.6, 4.7 the model overpredicts the concentration profile.

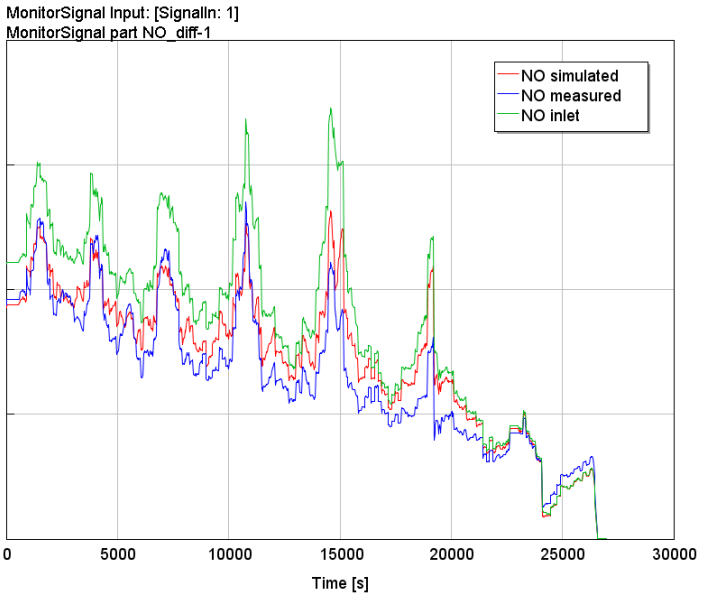

Figure 4.5: NOx flow along the reactor for a PLM dataset with SS tuned kinetic parameters

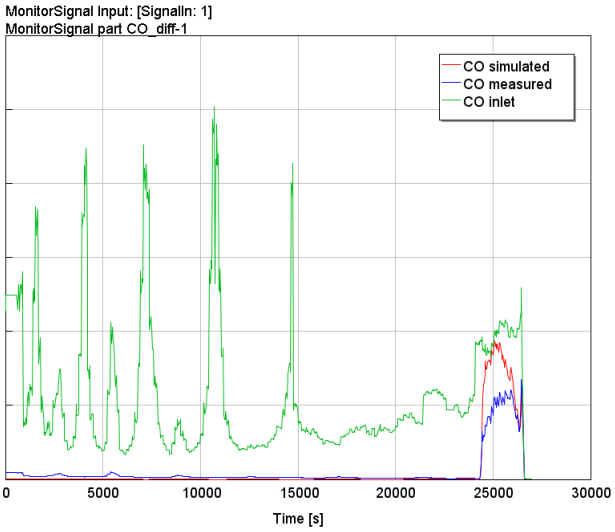

Figure 4.6: CO flow along the reactor for a PLM dataset with SS tuned kinetic parameters

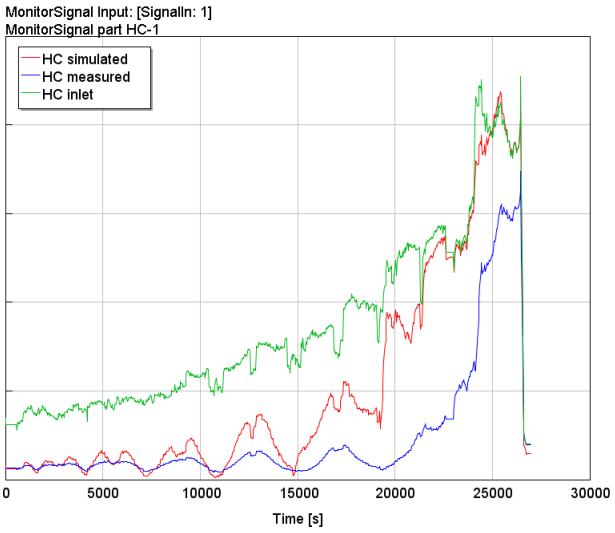

Figure 4.7: HC flow along the reactor for a PLM dataset with SS tuned kinetic parameters

4.4 Heat Transfer Model

A simple Matlab code was developed to determine the time lapse, τ taken by the inlet temperature to reach the same temperature in measured outlet. The matlab code and calculation method is shown in Appendix. The plot is shown in Fig 4.8 where it could be seen that there exists a vast time lag indicative of poor thermal

response of the model. Also, the peaks in time lags can be correlated with the rise in temperature error response as shown in Fig 4.9

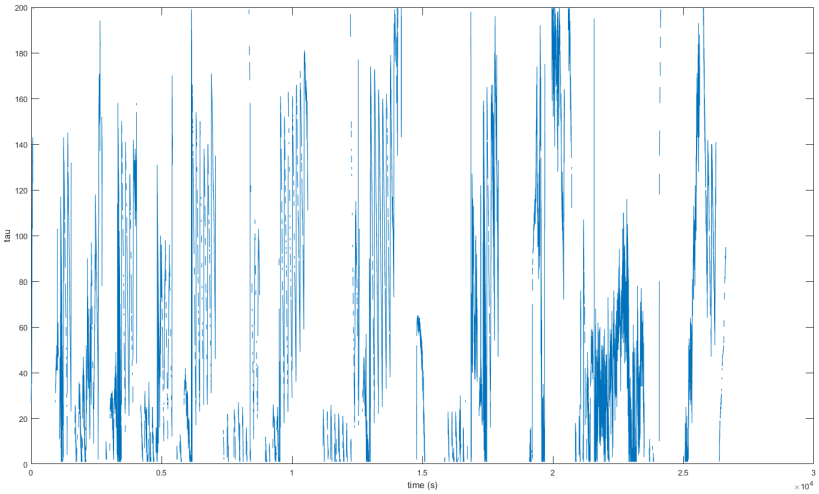

Figure 4.8: Thermal lag Time constant τ required for inlet temperature to reach the same outlet temperature

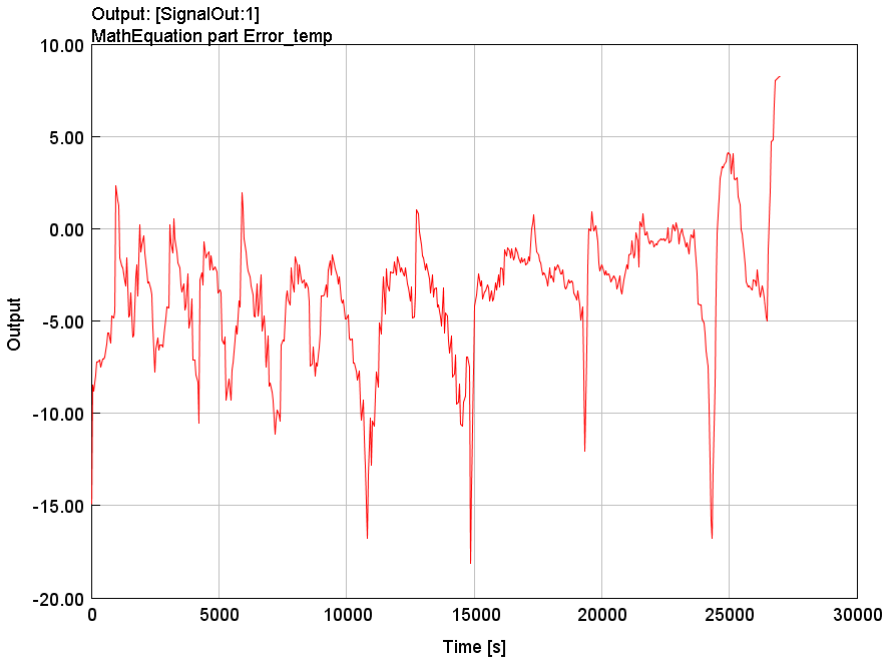

Figure 4.9: The error in temperature prediction for the PLM drive cycle

Hence, it was suspected that the 1D model was failing to capture thermal mass variations along the reactor. As we could see from Fig 4.10 the temperature prediction in C1 cycle not only is poor, but has random bumps in prediction. The wall

temperature solution in this case is automatically calculated by GT-Suite. From Fig 4.11 it could be seen that the reason for this sudden temperature shoot is because of the mismatch between exhaust gas temperature and solid internal wall temperature. In reality, when the hot exhaust gas flows through the reactor, there is thermalmass heat-up because of which the monolith wall temperature rises. Inturn, the catalyst wall convects heat through the insulation layers and also back into the reactor. In this case, the solid temperature is too low to retain enough heat and thus is the reason for the temperature lag observed earlier. The gas and the solid temperatures should hence follow the same pattern with a small shift in magnitude. This heat flow is clearly not understood by the 1D model. From Fig 4.11 it is clear that the solid temperature is very different from the gas temperature. This is indicative of poor heat transfer estimation by the model.

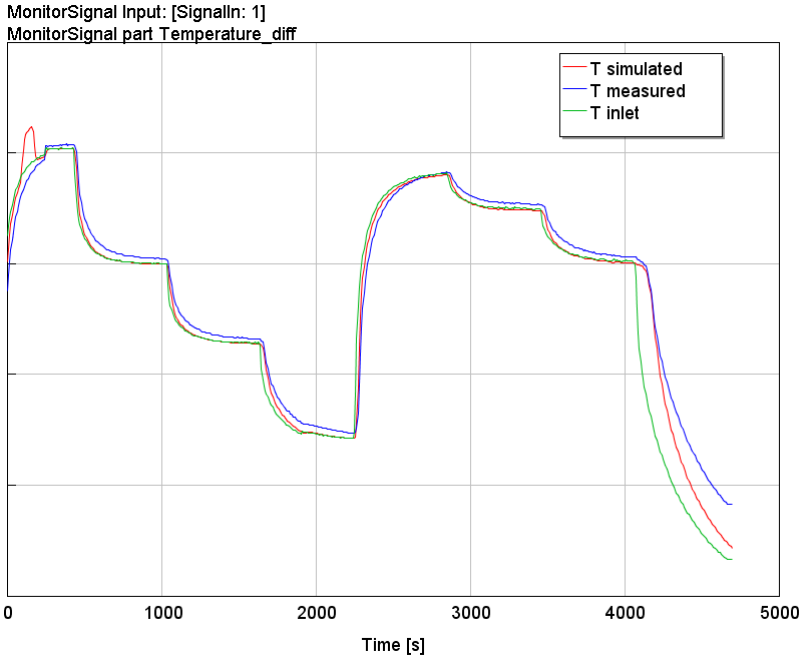

Figure 4.10: Temperature prediction for C1 drive cycle using the 1DOC 1brick model

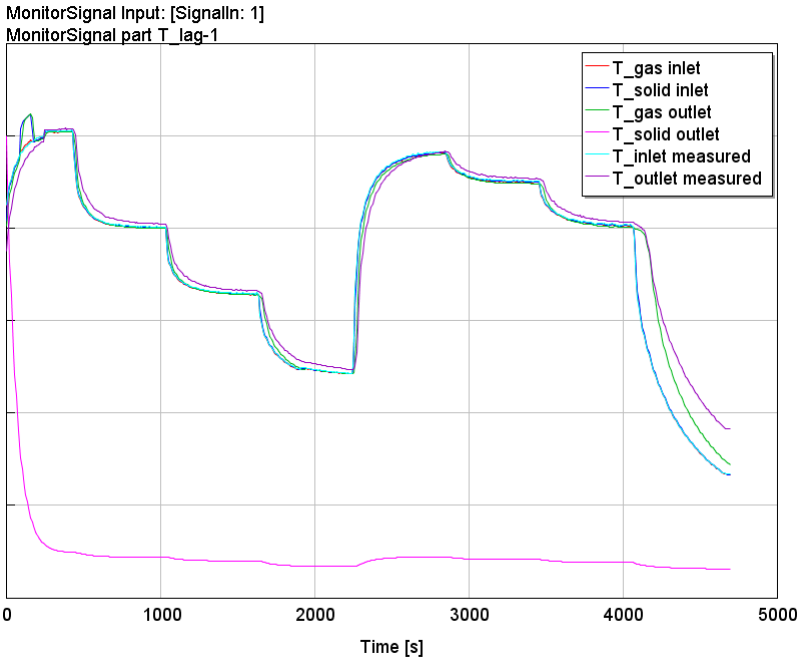

Figure 4.11: Temperatures of the catalyst wall and the exhaust gas for a C1 driving cycle

Inorder to account for this problem, a 2D model which would account for axial heat dispersion was developed. The discretization of individual tanks and the representation of individual thermal mass elements was believed to improve the thermal mass understanding and provide the user with more means of controlling the system.

Since the C1 drive cycle has sudden changes in temperature curves and the temperature difference between the inlet and measured was very small at most places, the C1 cycle was chosen to calibrate heat transfer parameters of this model. The major heat transfer parameters that were tuned were the specific heat of corderite, the heat transfer coefficient between all the thermal mass terms of the insulation layers (this is a single value, since the heat transfer coefficients between the thermal masses were the same) and the Heat Transfer coefficient multiplier between the gas phase and the solid wall.

A multi-objective parametric optimization was performed to minimize both the total temperature error and the temperature difference between the solid and the gas temperature. Evidently, from Fig 4.12 it could be seen that the temperature prediction has reasonably improved, most importantly the temperature lag between the solid and gas temperature has been resolved as shown in Fig 4.13 .

On re-optimizing the kinetic parameters, the species predictions have further improved since the reactions are highly temperature dependant.

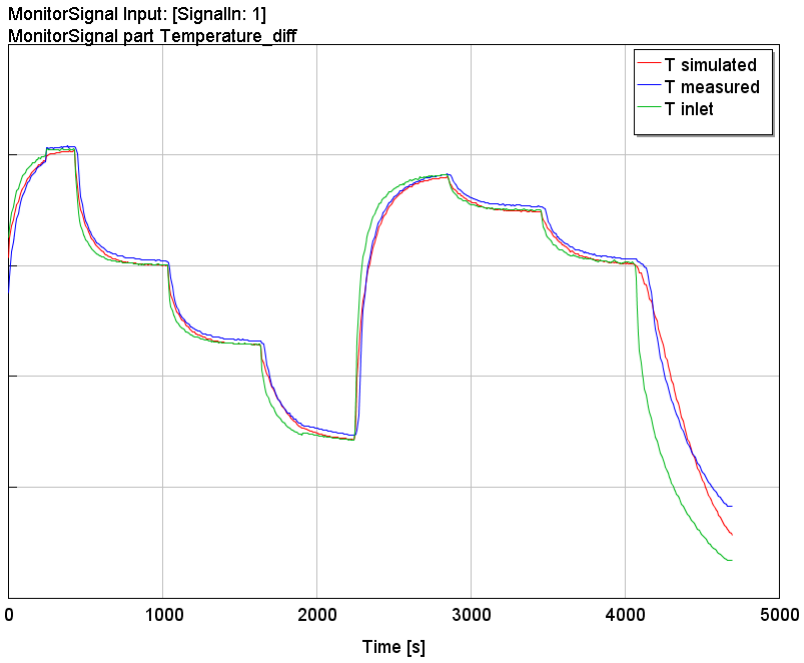

Figure 4.12: Temperature prediction for a C1 drive cycle using the improved 1 DOC thermal model

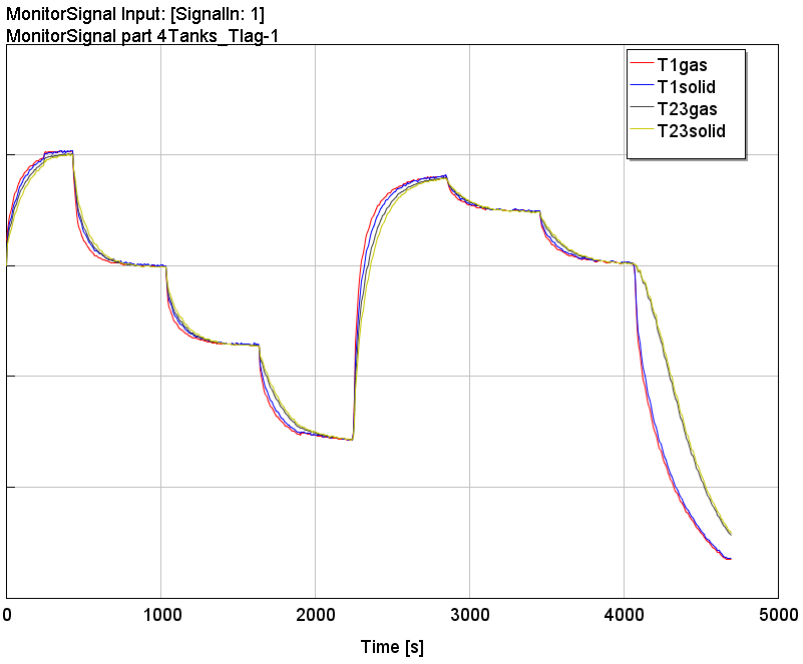

Figure 4.13: Solid and exhaust gas temperatures for the 1 DOC thermal model

Fig 4.14, 4.15, 4.16 shows the verification of the thermal model using the PLM dataset.

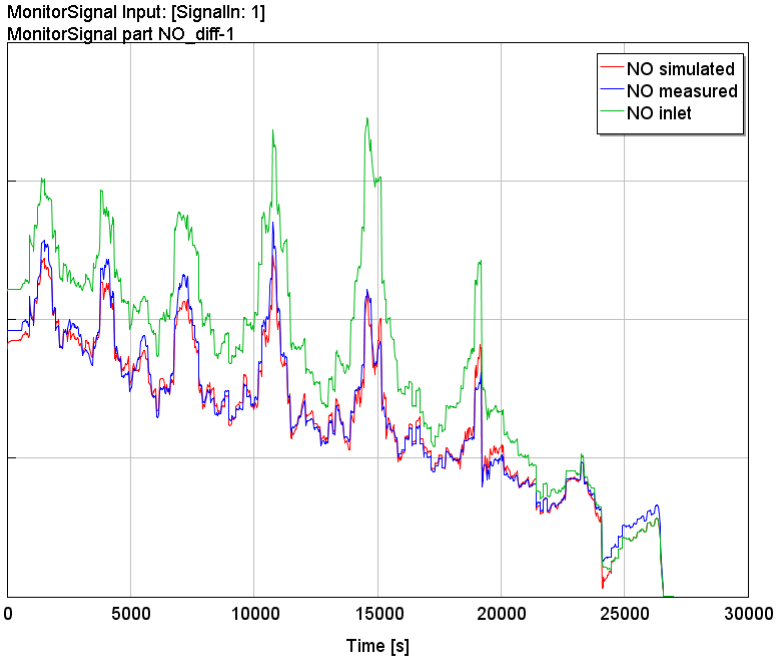

Figure 4.14: NO prediction for PLM drive cycle using the 1 DOC thermal model

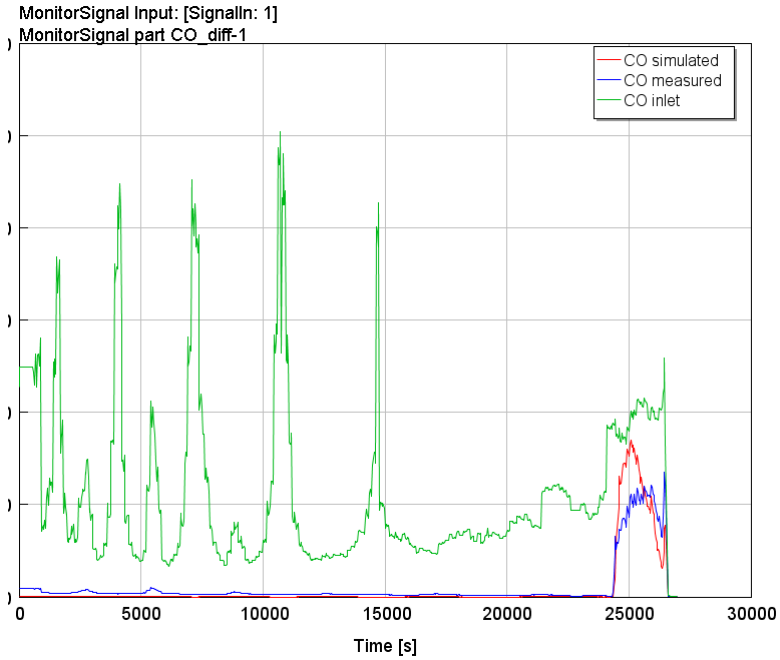

Figure 4.15: CO prediction for a PLM drive cycle using the 1 DOC thermal model

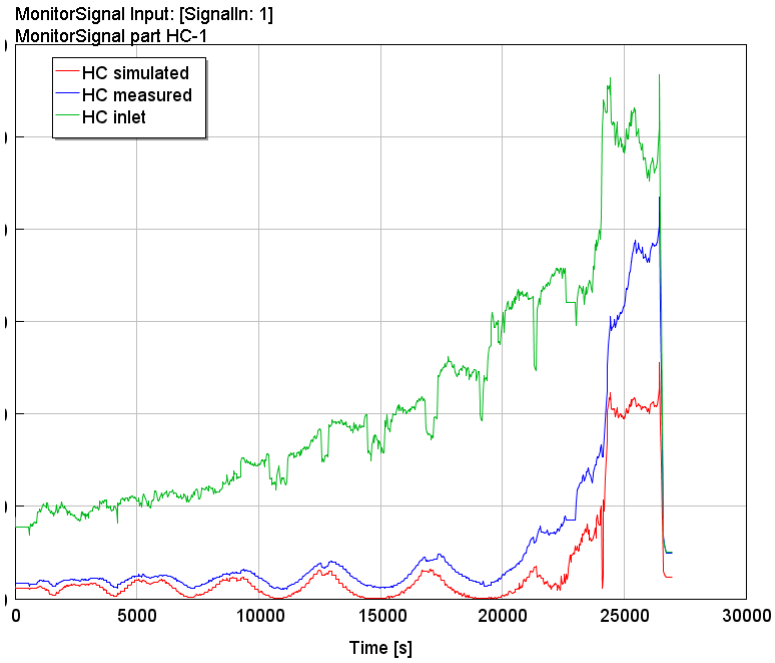

Figure 4.16: HC prediction for a PLM drive cycle using the 1 DOC thermal model

4.5 2 DOC Model

A similar approach was taken in the 2 DOC model, where the heat transfer parameters were optimized and later the reaction kinetics. After the parametric optimization, from Fig 4.17, 4.18 it could be observed that the temperature fit has slightly improved but the species prediction shown in Fig 4.19, 4.20, 4.21 are the same as for the 1 DOC model. This is probably because the mass flow distribution was handled much better by the model with the flow split factor α and continual heat exchange between the catalysts provides the model with more flexibility to solve thermal mass variations.

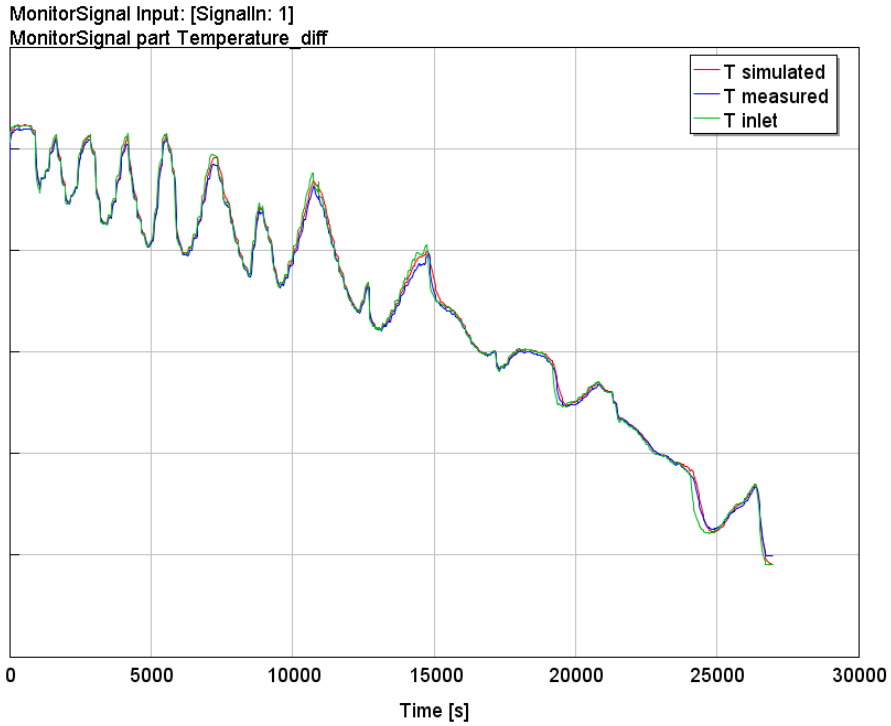

Figure 4.17: T prediction for PLM drive cycle using the 1 DOC thermal model

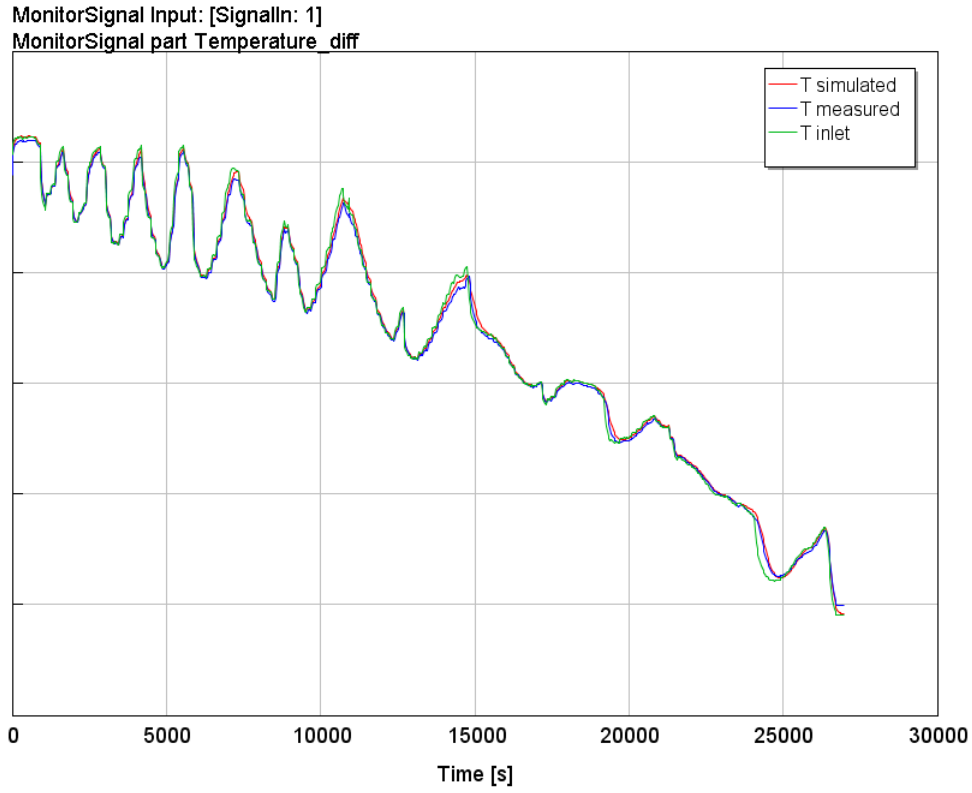

Figure 4.18: T prediction for PLM drive cycle using the 2 DOC thermal model

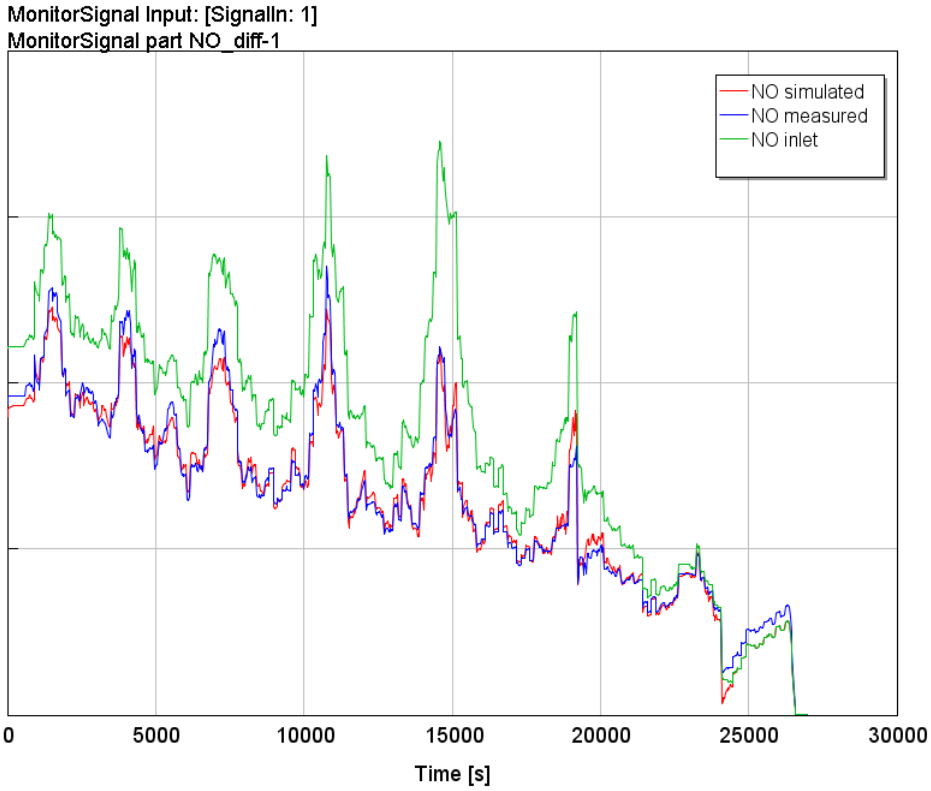

Figure 4.19: NO prediction for PLM drive cycle using the 2 DOC thermal model

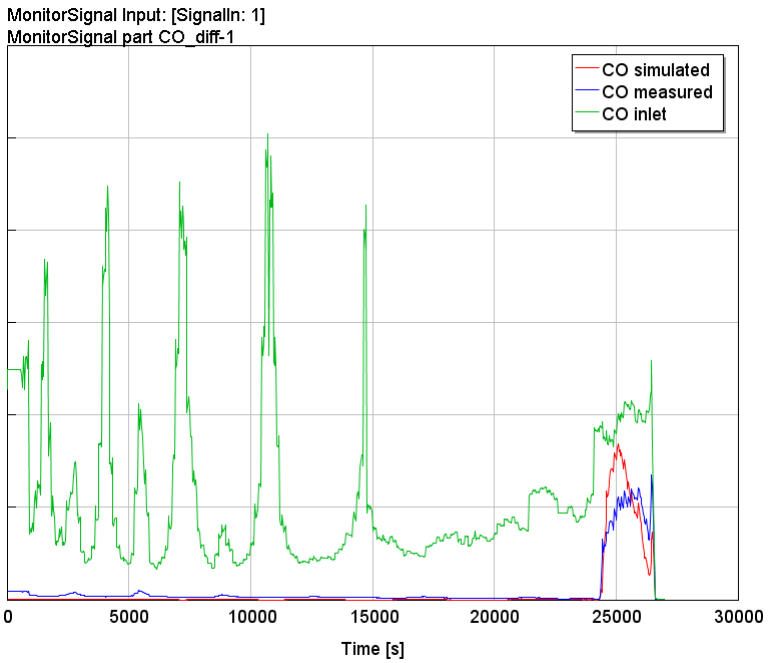

Figure 4.20: CO prediction for a PLM drive cycle using the 2 DOC thermal model

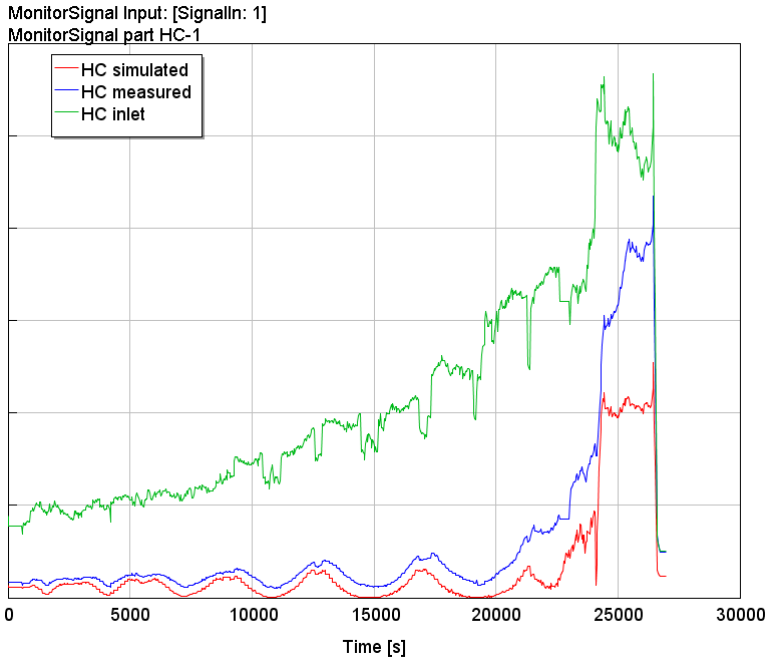

Figure 4.21: HC prediction for a PLM drive cycle using the 2 DOC thermal model

The 2 DOC model was developed to accurately understand the heat transport and flow behaviour of the system. Moreover, in the 2 DOC model, since the external heat transfer parameters were calibrated specifically for an individual subvolume of the whole reactor, it was anticipated that the solver would face a simpler problem than earlier models, which provides more scope for the model to resolve reaction parameters much more precise and efficient.

Although, on comparing the 1 and 2 DOC models, the 2 DOC model has the same predictability as the 1 DOC model interms of species concentration as shown in Table 4.2. The temperature prediction however has improved by a considerable amount. On the contrary, this model is also highly temperature sensitive and could cause thermal instability of thermal mass components in particular locations. A detailed investigation of where instabilities occur and the physical significance of the occurrence is up for future research. The 2 DOC model uses the RADAU solver which is robust but computationally expensive. The long simulation times makes this model less robust in terms of integrating with online fast running engine models, However the capacity of the model to account for varying flow regimes and thermal mass makes the model more reliable in terms of accuracy. Since it is uncertain as to why the species prediction of this model hasn't improved, without further research it is not possible to conclude on the reliability of this model.

Table 4.2: shows the reduction in total absolute error of species and temperature after each modelling approach for a PLM driving cycle

Species	Previous Work	Inhibition Function	1DOC HT model	2DOC HT model
CO	6.88 E-6	2.04 E-6	1.42 E-6	1.43 E-6
HC	1.21 E-5	1.06 E-5	1.65 E-7	1.64 E-7
NO	8.19 E-4	5.33 E-5	3.55 E-5	3.20 E-5
Temperature	731831	634336	425347	343430

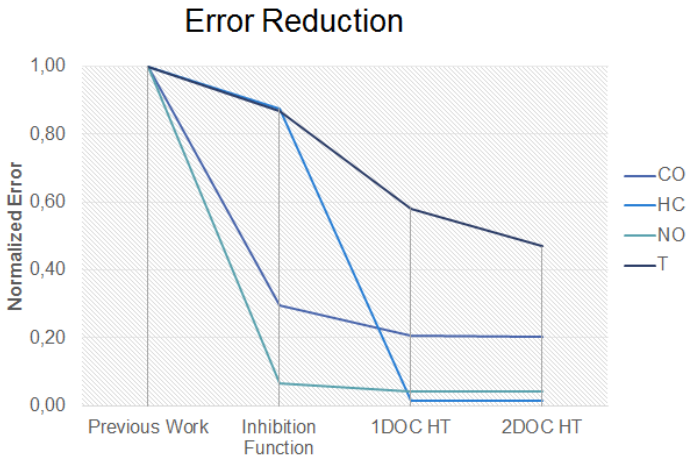

Figure 4.22: Normalized absolute error for a PLM driving cycle after each modelling step

4.6 Model Validation

One of the key objectives of this thesis work was to develop a consistent model that would be capable of giving the similar performance with all drive cycles. The model was hence validated with an NRTC drive cycle. Figures 4.23,4.24,4.25 shows the species prediction using the 1 DOC models. On comparing with results from Almqvist [1], it could be clearly seen that the prediction accuracy for HC and NOx have vastly increased.

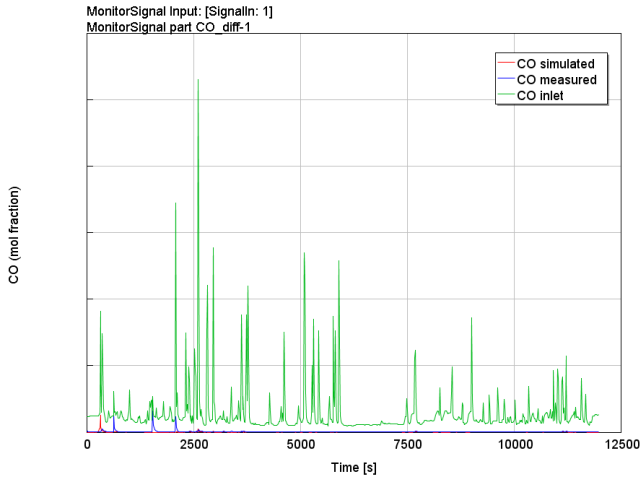

Figure 4.23: CO prediction for a NRTC drive cycle using the 1 DOC thermal model

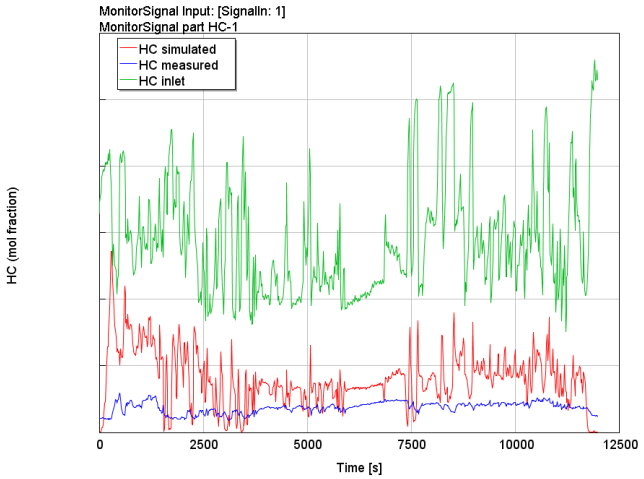

Figure 4.24: HC prediction for a NRTC drive cycle using the 1 DOC thermal model

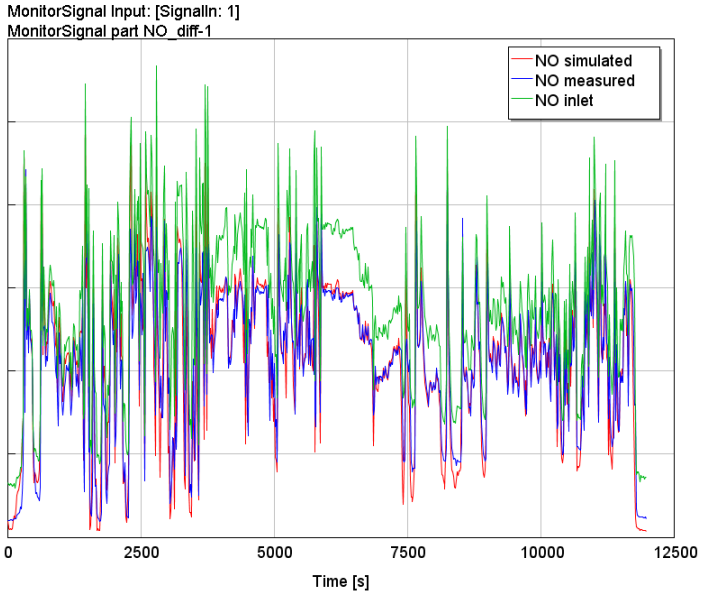

Figure 4.25: NO prediction for a NRTC drive cycle using the 1 DOC thermal model

On looking at the temperature prediction in Fig 4.26, a lag still exists. The temperature predictability of the 1 DOC model for the NRTC drive cycle is the exact same as Fig 4.26. On detailed observation, it could be seen that the temperature response and pattern of the inlet curve and the measured outlet curves are very different. There seems to be a lag in temperature response and the sharp peaks are not followed by the measured outlet curve at all. The model uses the inlet temperature as a basis for temperature prediction and hence the simulated temperature has a similar pattern to that of the inlet. So, this lag that is observed could be because of the measurement sensor at the outlet. It is possible that the nature of the sensor is that it doesn't capture sharp variations in temperature. Further, it could also be because of the fact that there could be good mixing for a drive cycle like NRTC.

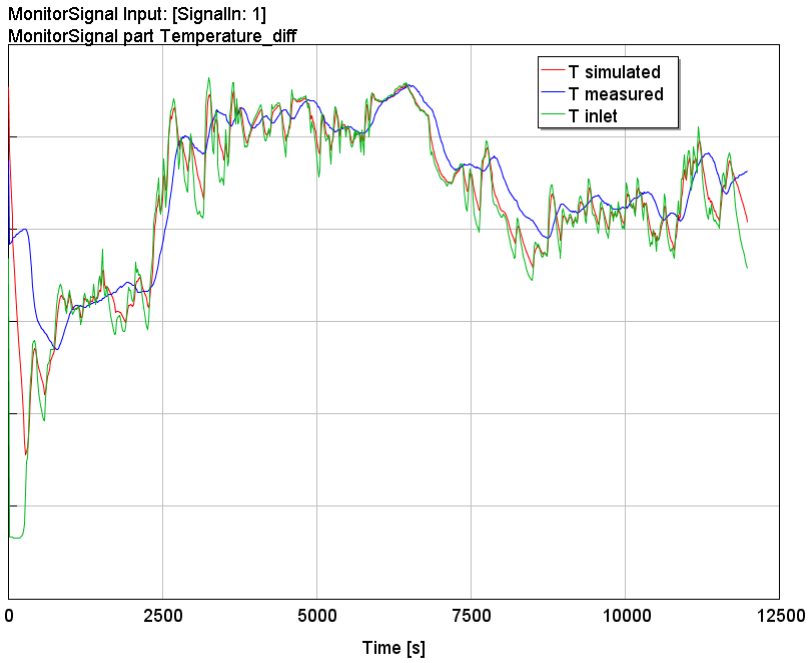

Figure 4.26: T prediction for a NRTC drive cycle using the 2 DOC thermal model

Conclusion

Common assumptions made in developing 1D reactor models are flow uniformity and negligible axial temperature gradient. These are serious assumptions that would severely affect the accuracy and consistency of the model. Hence, 1D models in general would be less reliable for modelling purposes. As discussed in this thesis, a semi-physical 2D model can possibly perform well and provide more control over EATS modelling.

The 2 DOC model has to be further investigated in terms of physical and numerical behaviour. The physical correlation of the distribution factor α has to be further understood. The reduction in temperature error by the 2 DOC model proves further scope for optimizing the predictability of the 2 DOC model.

For future measurements, both the gas temperature and the wall temperature could be measured to understand the effect of wall temperature on the model and between different drive cycles.

Simulation was performed on NRTC dataset from different test rigs, however the same type of prediction error in temperature was noticed. The exact nature of this problem is not completely known and would be an interesting avenue to investigate in future studies.

Bibliography

[1] Frida Almqvist. Combined Empirical and 1D Modeling Approach for Exhaust Aftertreatment System for Heavy. *Department of Applied Mechanics*, 81:1–81, 2017.

[2] Hongda Cen. Calibration and validation of 1D Diesel Oxidation Catalyst and Particulate Filter model in Heavy Duty Diesel Engines. *Department of Mechanics and Maritime Sciences*, 81:1–81, 2018.

[3] European Commission. Regulation (EU) 2016/1628 Of The European Parliament And Of The Council Of 14 September 2016. *Euratom*, 2016(167), 2016.

[4] Friedrich Forsthuber, Thorsten Krenek, Franz Marinitsch, Thomas Lauer, Joachim Weiss, Markus Raup, and Thorolf Schatzberger. Investigations on the Tail-Pipe Emissions of Commercial Engines with Advanced One-Dimensional Simulation Methods. 2013.

[5] Olivier Lepreux, Yann Creff, and Nicolas Petit. Model-based control design of a diesel oxidation catalyst. *IFAC Proceedings Volumes*, 42(11):279 – 284, 2009. 7th IFAC Symposium on Advanced Control of Chemical Processes.

[6] April Russell and William S. Epling. Diesel oxidation catalysts. *Catalysis Reviews*, 53(4):337–423, 2011.

[7] Potente and L Daniel. General design principles for an automotive muffler potente. 2005.

[8] Martin Williams and Ray Minjares. A technical summary of euro 6/vi vehicle emission standards. *The International Council on Clean Transportation (ICCT)*, (6):12, 2016.

[9] Andrew Pedlow, Geoffrey Mccullough, Alexandre Goguet, Ken Hansen, and Jaguar Land Rover. Optimization of Kinetic Parameters for an Aftertreatment Catalyst. 2015.

[10] S Katare and P Laing. A Hybrid Framework for Modeling Aftertreatment Systems: A Diesel Oxidation Catalyst Application. *SAE International*, 2006(2006-01-0689):10, 2006.

[11] Weiyong Tang, Syed Wahiduzzaman, Seth Wenzel, Andy Leonard, and Thomas Morel. Development of a Quasi-Steady Approach Based Simula-

tion Tool for System Level Exhaust Aftertreatment Modeling. *Sae Technical Paper Series*, 2008(724):776–790, 2008.

[12] Pinder K. L. Fogler, h. s. "elements of chemical reaction engineering", prentice-hall, englewood cliffs, new jersey 07632, 1986, 769 pages. *The Canadian Journal of Chemical Engineering*, 65(3):526–527.

[13] Gamma Technologies. Exhaust aftertreatment application manual. VERSION 2018:1–156.

[14] Sterling E. Voltz, Charles R. Morgan, David Liederman, and Solomon M. Jacob. Kinetic study of carbon monoxide and propylene oxidation on platinum catalysts. *Product R&D*, 12(4):294–301, 1973.

[15] M. Khosravi, A. Abedi, R.E. Hayes, W.S. Epling, and M. Votsmeier. Kinetic modelling of pt and pt:pd diesel oxidation catalysts. *Applied Catalysis B: Environmental*, 154-155:16 – 26, 2014.

[16] Chaitanya S. Sampara, Edward J. Bissett, Matthew Chmielewski, and Dennis Assanis. Global kinetics for platinum diesel oxidation catalysts. *Industrial & Engineering Chemistry Research*, 46(24):7993–8003, 2007.

[17] Tian Gu and Vemuri Balakotaiah. Analysis of upstream creeping reaction zones in catalytic monolith reactors. *Chemical Engineering Journal*, 317:267 – 279, 2017.

[18] Jonathan E. Etheridge and Timothy C. Watling. Is reactor light-off data sufficiently discriminating between kinetic parameters to be used for developing kinetic models of automotive exhaust aftertreatment catalysts? the effect of hysteresis induced by strong self inhibition. *Chemical Engineering Journal*, 264:376 – 388, 2015.

Appendix

A.0.1 Results from Almqvist [1]

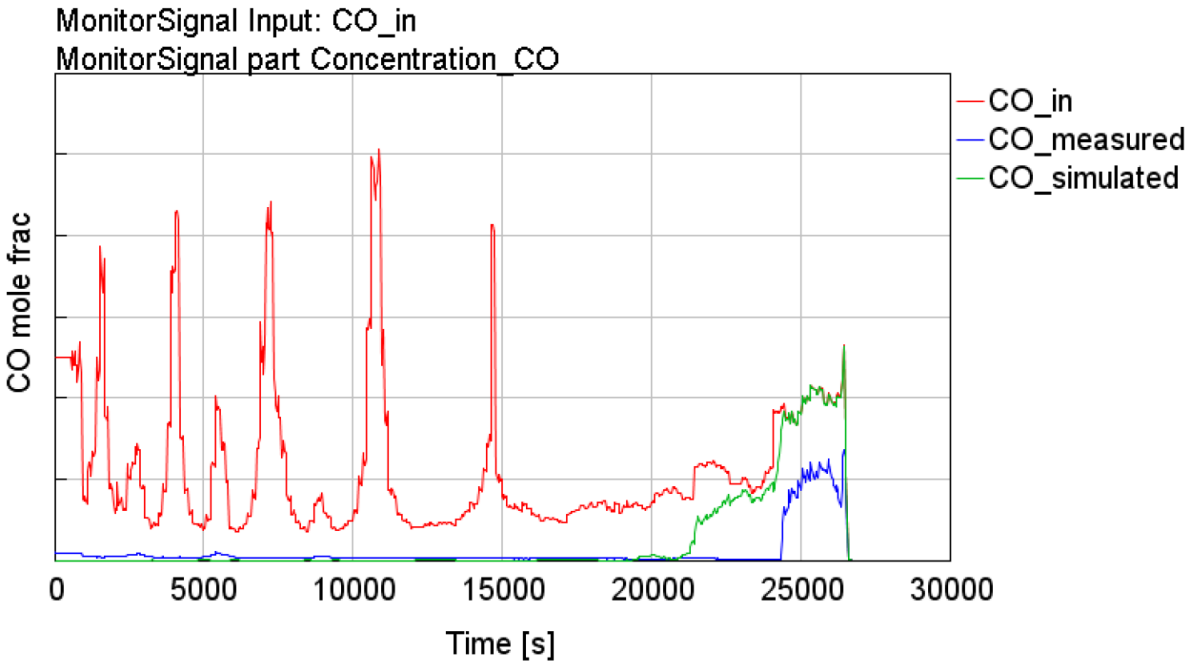

Figure A.1: CO flow for a PLM drive cycle from Almqvist´s [1] model

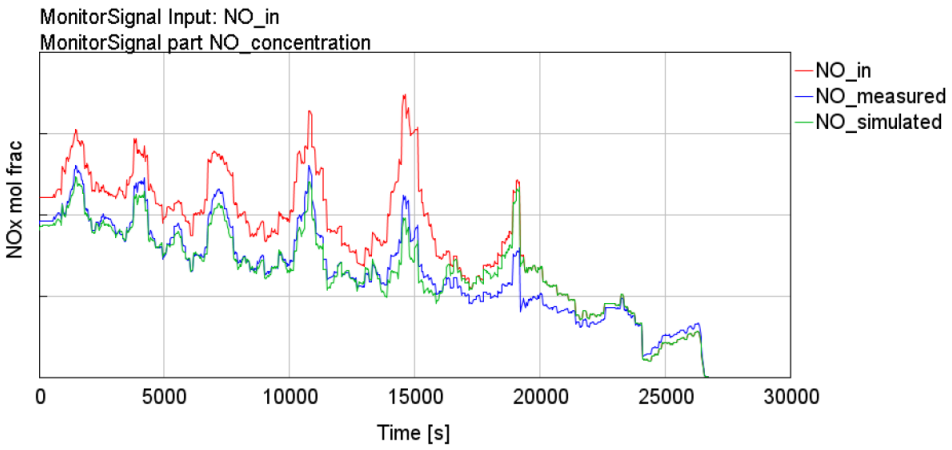

Figure A.2: NO flow for a PLM drive cycle from Almqvist´s [1] model

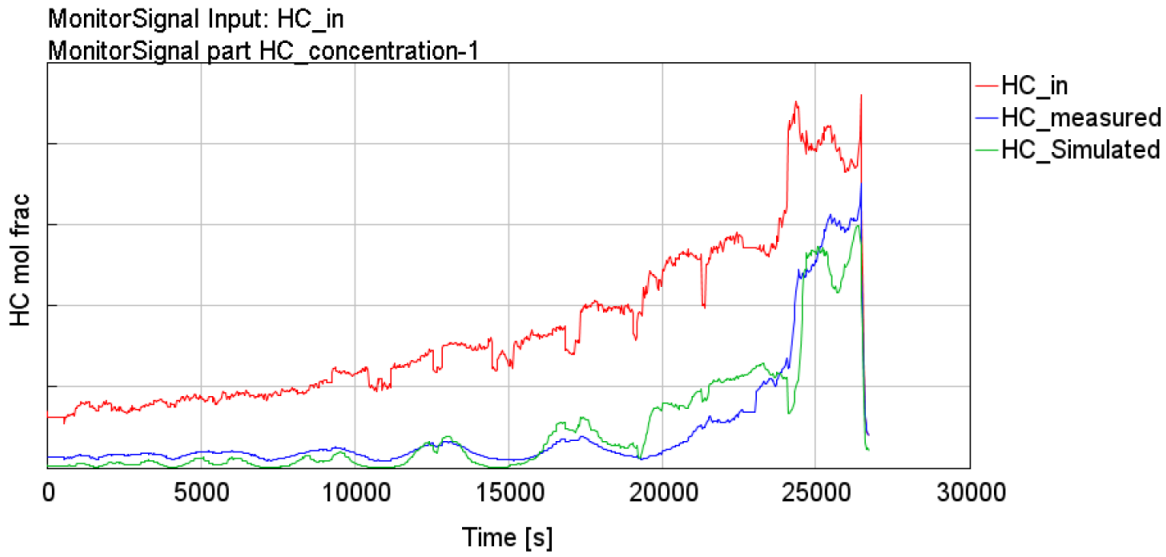

Figure A.3: HC flow for a PLM drive cycle from Almqvist´s [1] model

A.0.2 Results from Cen [2]

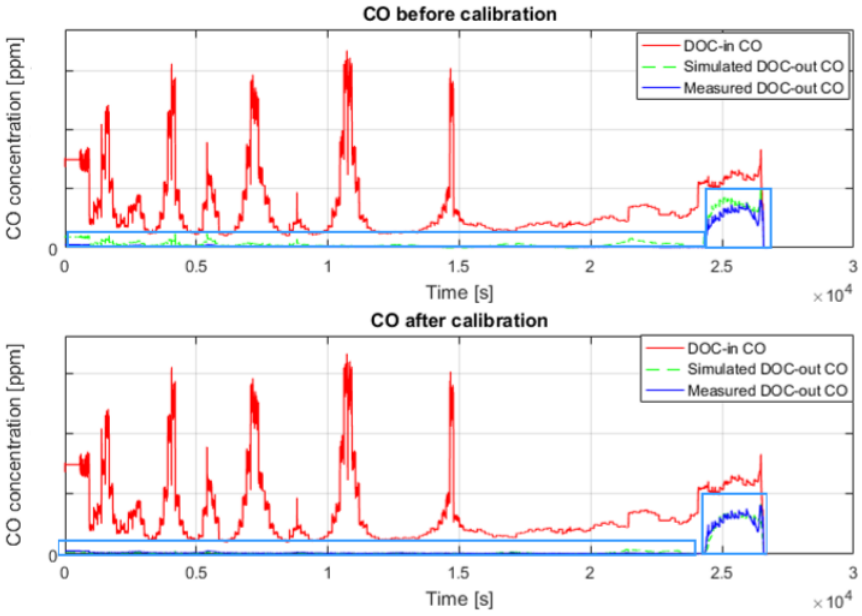

Figure A.4: CO flow for a PLM drive cycle from Cen´s [2] model

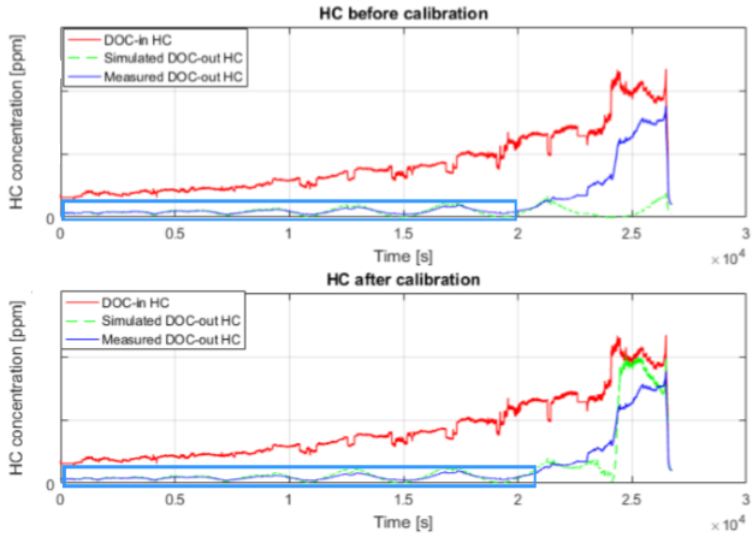

Figure A.5: HC flow for a PLM drive cycle from Cen´s [2] model

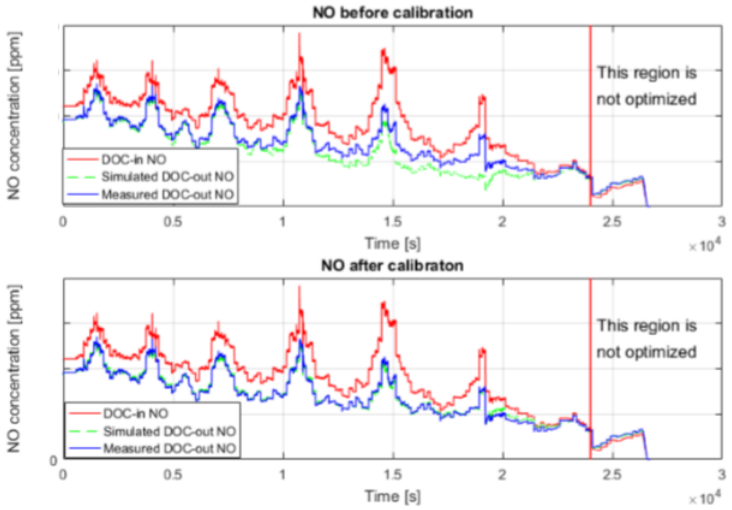

Figure A.6: NO flow for a PLM drive cycle from Cen´s [2] model

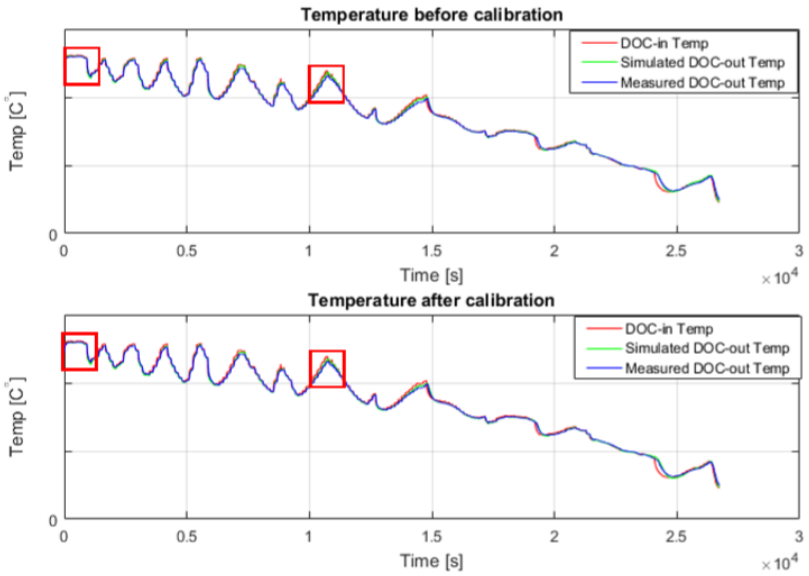

Figure A.7: Temperature for a PLM drive cycle from Cen´s [2] model

A.0.3 Matlab Program

A matlab code was developed to determine the time lag τ. The inlet and measured outlet data are first imported to the matlab workspace. Inlet and outlet temperatures are assigned to a vector. A variable was defined to specify the search duration which would dictate the resolution of the search region. The code will check if the difference between an inlet value and 500 consecutive measured value is 0. This will be performed by the means of a for loop and is calculated for every single inlet data point. If there exists a difference between inlet and measured values, the time taken for the inlet value to reach the corresponding measured value is determined and stored into a new variable named temp. If the program cannot find the corresponding measured temperature for a stipulated inlet temperature, then it treated as 'NaN'. This is because, there exists a lag and increasing the search space further would only give us wrong results since on further search the inlet temperature would eventually match a measured temperature of a different region. The temp variable measured is the time lag τ and is plotted against the time series of the dataset.

```
clc
clear
close all

disp('Loading data...')
searchduration=500; %determines the resolution of the search space

%% PLM
% indata=xlsread('PLM.xlsx','Inlet_mol fraction');
% outdata=xlsread('PLM.xlsx','OUT');
%
% T_in=indata(:,2);
% T_out=outdata(:,1);
% m_in=indata(:,4);
% tottime=12563;

% time=[1:tottime];
% time=[1:26725];
% time=time';

%% NRTC
indata=xlsread('NRTC_aged.xlsx','In'); % reads inlet data
outdata=xlsread('NRTC_aged.xlsx','Out'); % reads measured data

T_in=indata(:,2); % reads temperature from inlet data
T_out=outdata(:,2); % reads temperature from measured data
m_in=indata(:,4); % reads inlet mass flow from inlet data
tottime=12563; % total test time in the drive cycle
T_in(tottime+1:tottime+searchduration)=0;
T_out(tottime+1:tottime+searchduration)=0;
m_in(tottime+1:tottime+searchduration)=0;

time=[1:tottime];
time=time';

%%

temp=0;

for i=1:1:tottime % for loop to compare every inlet data point from 1
till the end of the dataset
    for j=i:1:i+searchduration % compares each inlet data point with
500 consecutive measured data points
    if abs(T_in(i)/T_out(j)-1)<0.0005 % if the difference is ~0, then
there is no lag
        temp(j)=time(j); % if it is >0, the lag time is determined and
stored
    end
    end
    res=min(nonzeros(temp));
    temp=9999999;
    tau(i)=res-i;
```

```
    if tau(i)>5000 || tau(i)==0
        tau(i)=NaN;
    end
    i
end

figure
s=size(tau);
time=[1:s(2)];
plot(time,tau)
xlabel('time (s)')
ylabel('tau')

figure
plot(m_in(1:s(2)),tau,'.')
xlabel('massflow (kg/s)')
ylabel('tau')
```